The small G-protein Rac1 in the dorsomedial striatum promotes alcohol-dependent structural plasticity and goal-directed learning in mice

Zachary W. Hoisington[1], Alexandra Salvi[1], Sophie Laguesse[2], Yann Ehinger[1], Chhavi Shukla[1], Khanhky Phamluong[1], and Dorit Ron[1]

[1]Alcohol and Addiction Research Group, Department of Neurology, University of California San Francisco, USA, 94107; [2]GIGA-Stem Cells and GIGA-Neurosciences, Interdisciplinary Cluster for Applied Genoproteomics (GIGA-R), University of Liège, Belgium

*Correspondence: D. Ron, Department of Neurology, University of California, San Francisco, 675 Nelson Rising Lane, BOX 0663, San Francisco, CA 94143-0663, USA. dorit.ron@ucsf.edu

51 pages

10 Figures, 3 Extended Figures, 1 table

Abstract: 243 words

Introduction: 570 words

Discussion: 1492 words

Abbreviated title: Rac1 and alcohol

Acknowledgements: This study was funded by National Institute of Alcohol Abuse and Alcoholism R01 AA027682 (DR). BioRender.com. was used to create some of the figures. ZWH was partially funded by NIH GM007175.

The authors have no conflict of interest.

Abstract

The small G-protein Rac1 promotes the formation of filamentous actin (F-Actin). Actin is a major component of dendritic spines, and we previously found that alcohol alters actin composition and dendritic spine structure in the nucleus accumbens (NAc) and the dorsomedial striatum (DMS). To examine if Rac1 contributes to these alcohol-mediated adaptations, we measured the level of GTP-bound active Rac1 in the striatum of male and female mice following 7 weeks of intermittent access to 20% alcohol. We found that chronic alcohol intake activates Rac1 in the DMS, but not in the NAc and DLS of male mice. Chronic excessive alcohol intake does not activate Rac1 in the DMS of female mice. Similarly, closely related small G-proteins are not activated by alcohol in the DMS, and Rac1 activity is not increased in the DMS by moderate alcohol or natural reward. To determine the consequences of alcohol-dependent Rac1 activation in the DMS of male mice, we inhibited endogenous Rac1. We infected the DMS of mice with an AAV expressing a dominant negative form of the small G-protein (Rac1-DN). We found that overexpression of AAV-Rac1-DN in the DMS inhibits alcohol-mediated Rac1 signaling and attenuates alcohol-mediated F-Actin polymerization, which corresponded with a decrease in dendritic arborization and spine maturation. Finally, we provide evidence to suggest that Rac1 in the DMS plays a role in alcohol-associated goal-directed learning. Together, our data suggest that Rac1 in the DMS plays an important role in alcohol-dependent structural plasticity and aberrant learning.

47 **Significance Statement**

48 Addiction, including alcohol use disorder, is characterized by molecular and cellular
49 adaptations that promote maladaptive behaviors. We found that Rac1 was activated by alcohol in
50 the dorsomedial striatum (DMS) of male mice. We show that alcohol-mediated Rac1 signaling is
51 responsible for alterations in actin dynamics and neuronal morphology. We also present data to
52 suggest that Rac1 is important for alcohol-associated learning process. These results suggest
53 that Rac1 in the DMS is an important contributor to adaptations that promote alcohol use disorder.
54

55 **Introduction**

56 Rac1 (Ras-related C3 botulinum toxin substrate 1) is a small G-protein belonging to the
57 Rho family of GTPases (Van Aelst and D'Souza-Schorey, 1997; Vetter and Wittinghofer, 2001;
58 Bosco et al., 2009). Rac1 is expressed ubiquitously and plays a role in processes such as actin
59 polymerization, endocytosis, transcription, and cell growth (Nakayama et al., 2000; Ridley, 2006;
60 Bosco et al., 2009). Rac1 is highly expressed in the central nervous system (CNS) (Corbetta et
61 al., 2009). Rac1 cycles between a GDP-bound inactive state and a GTP-bound active state
62 (Vetter and Wittinghofer, 2001). In the CNS, the transition between GDP-bound to GTP-bound
63 Rac1 is catalyzed by the guanine nucleotide-exchange factors (GEFs) Tiam1 and Karilin-7 (Vetter
64 and Wittinghofer, 2001; Tolias et al., 2005; Xie et al., 2007). The Rac1 GTPase activating proteins
65 (GAPs), such as RacGAP1 or FilGAP (Toure et al., 1998; Nguyen et al., 2018), initiate the intrinsic
66 GTPase activity of Rac1 resulting in the conversion of GTP to GDP (Vetter and Wittinghofer,
67 2001). Upon activation, Rac1 binds to p21-activated kinase (PAK1) leading to PAK1
68 autophosphorylation and activation (Bokoch, 2003). PAK1 phosphorylates and activates LIM
69 kinase (LIMK) (Edwards et al., 1999). LIMK then phosphorylates cofilin (Yang et al., 1998;
70 Bernard, 2007; Scott and Olson, 2007). Cofilin's function is to sever actin filaments (F-actin) into
71 globular actin (G-actin) (Yang et al., 1998; Bamburg, 1999; Maciver and Hussey, 2002;
72 Andrianantoandro and Pollard, 2006; Chin et al., 2016; Kanellos and Frame, 2016). LIMK
73 phosphorylation of cofilin prevents cofilin's ability to cleave actin, therefore enabling the formation
74 and maintenance of F-actin (Yang et al., 1998; Pavlov et al., 2007; Scott and Olson, 2007). This
75 mechanism promotes spine enlargement and stabilizes and strengthens synapses (Honkura et
76 al., 2008; Chazeau and Giannone, 2016; Costa et al., 2020). As such, Rac1 is involved in long-
77 term potentiation, the cellular mechanism of learning and memory (Haditsch et al., 2009; Haditsch
78 et al., 2013; Lv et al., 2019).

79 Malfunction of Rac1 has been associated with multiple neurological and psychiatric
80 disorders. For example, abnormal expression of Rac1 has been observed in humans suffering

81 from schizophrenia, autism spectrum disorders, and fragile X syndrome (Tejada-Simon, 2015;
82 Reijnders et al., 2017; Wang et al., 2020). A reduction of Rac1 expression is also associated with
83 stress, depression, and anhedonia in mice (Golden et al., 2013), symptoms that often coincide
84 with addiction (Koob and Kreek, 2007). Abnormal Rac1 function has been linked to drugs of
85 abuse. Specifically, Rac1 activity is inhibited after repeated, but not acute, cocaine administration
86 in the NAc of mice (Dietz et al., 2012), and Rac1-dependent mechanisms affect the extinction of
87 aversive opiate withdrawal memories (Wang et al., 2017). Finally, Rac1 orthologs have been
88 shown to regulate ethanol acute sensitivity in *Drosophila melanogaster* (Peru et al., 2012).
89 However, Rac1's function in alcohol use disorder (AUD) has not been investigated in a
90 mammalian system.

91 Previously, we found that excessive chronic alcohol consumption promotes the formation
92 of F-actin in the NAc (Laguesse et al., 2017) and in the dorsomedial striatum (DMS) of mice
93 (Wang et al., 2015; Laguesse et al., 2018). We further found that heavy alcohol consumption in
94 mice results in a structural remodeling in both brain regions, leading to the maturation of dendritic
95 spines in the NAc and in the branching of dendrites and remodeling of dendritic spines in DMS
96 (Wang et al., 2015; Laguesse et al., 2018). Here, we examined the possibility that Rac1 controls
97 these alcohol-dependent structural adaptations in the NAc and/or the DMS.

98 **Materials and Methods**

99 **Antibodies**

100 Rabbit anti-pLIMK (#ab38508) antibodies were purchased from Abcam (Waltham, MA). Chicken
101 anti-GFP (#A10262) antibodies were purchased from Life Technologies (Carlsbad, CA). Rabbit
102 anti-LIMK1 (#3842S), Cofilin (#3312S), pCofilin Ser3 (#3311S), RhoA (#6789S), Cdc42 (#2246S)
103 antibodies were purchased from Cell signaling technology (Danvers, MA). Mouse anti-GAPDH
104 (#G8795) antibodies, anti-actin (#A2228) antibodies, phosphatase inhibitor Cocktails 2 and 3
105 were from Sigma Aldrich (St. Louis, MO). Mouse anti-Rac1 antibodies (#ARC03), the G-Actin/F-
106 Actin assay kit (BK037), the Rac1 pull-down activation assay kit (#BK035), the RhoA pull-down
107 activation assay kit (#BK036), and the Cdc42 pull-down activation assay kit (#BK034) were
108 purchased from Cytoskeleton, Inc. (Denver, CO). Nitrocellulose membranes and Enhance
109 Chemiluminescence (ECL) were purchased from Millipore (Burlington, MA). EDTA-free complete
110 mini–Protease Inhibitor Cocktails were from Roche (Indianapolis, IN). Pierce bicinchoninic acid
111 (BCA) protein assay kit was purchased from Thermo Scientific (Rockford, IL). Ethyl alcohol (190
112 proof) was purchased from VWR (Radnor, PA). NuPAGE Bis-Tris precast gels were purchased
113 from Life Technologies (Carlsbad, CA). Donkey anti-rabbit horseradish peroxidase (HRP) and
114 donkey anti-mouse HRP conjugated secondary antibodies were purchased from Jackson
115 ImmunoResearch (West Grove, PA). The donkey anti-mouse IgG AlexaFluor 564 and donkey
116 anti-chicken AlexaFluor 488 antibodies were purchased from Life Technologies (Carlsbad, CA).

117

118 **Animals**

119 Male and female C57BL/6J mice (Jackson Laboratory, Bar Harbor, ME) arrived at 6-8 weeks old
120 and were allowed one week of habituation before experiments began. Mice were housed
121 individually in a reversed 12-hour light-dark cycle room (lights on at 22:00/off at 10:00) that was
122 temperature- and humidity-controlled. Unrestricted amounts of food and water were provided.

123 Animal procedures were approved by the UCSF Institutional Animal Care and Use Committee
124 (IACUC).
125
126 **Preparation of solutions**
127 Alcohol solution was prepared from an absolute anhydrous alcohol solution (190 proof) diluted to
128 20% (v/v) in tap water for alcohol-drinking experiments. Sucrose solution (1%) was dissolved in
129 tap water (w/v).
130
131 **Collection of brain samples for biochemical analyses**
132 Mice were euthanized 4 hours after the beginning of the last drinking session ("binge" timepoint)
133 or 24 hours after the last drinking session ("withdrawal" timepoint). Brains were removed and
134 dissected on an ice-cold platform into 1mm sections, and specific subregions were dissected
135 based on Allen Brain Atlas anatomy.
136
137 **Western blot analysis**
138 Tissue was homogenized in ice-cold radio immunoprecipitation assay (RIPA) buffer (in mM: 50
139 Tris-HCL, 5 EDTA, 120 NaCl, and 1%NP-40, 0.1% deoxycholate, 0.5% SDS, proteases and
140 phosphatases inhibitors). Samples were homogenized using a sonic dismembrator. Protein
141 content was determined using BCA™ protein assay kit. Thirty µg of each tissue lysate was loaded
142 for separation by SDS-PAGE then transferred onto nitrocellulose membrane at 300mA for 2
143 hours. Membranes were blocked with 5% milk-PBS containing 0.1% Tween 20 at room
144 temperature (RT) for 30 minutes and then probed with the appropriated primary antibodies
145 overnight at 4ºC. The membranes were washed and probed with HRP-conjugated secondary
146 antibodies for one hour at room temperature. Membranes were developed using the enhanced
147 chemiluminescent reagent (ECL) and band intensities were quantified using ImageJ software
148 (NIH).

149 **Small G-protein activation assay**

150 Small G-protein activity was determined using the Rac1, RhoA, or Cdc42 activation *in vivo* assay
151 biochemical kits for the respective protein (Cytoskeleton Inc., Denver, CO). The tissues were
152 lysed in lysis buffer (50mM Tris-HCl pH7.4, 450mM NaCl, 1% Triton X-100) containing protease
153 and phosphatase inhibitor cocktail. Thirty µg of each lysate was incubated with 10 µL PAK
154 Rac1/Cdc42 binding domain (PAK-PBD)-agarose beads for Rac1 and Cdc42, or 15 µL Rhotekin
155 Rho binding domain (Rhotekin-RBD)-agarose beads for RhoA, for 16 hours. For the control, the
156 same amount of lysate was incubated with GDP or GTP for 15 minutes followed by incubation
157 with PAK-PBD or Rhotekin-RBD-agarose beads for 16 hours. The beads were washed twice with
158 washing buffer followed by boiling in 30 µL 2X sample loading buffer. The samples were analyzed
159 by western blot.

160

161 **F-actin/G-actin assay**

162 F-actin and G-actin content was measured using the G-actin/F-actin in vivo assay biochemical kit
163 (Cytoskeleton Inc., Denver, CO) as previously described in (Laguesse et al., 2018) with slight
164 modification. Tissue punches were homogenized in 250 µL cold LAS02 buffer containing protease
165 and phosphatases inhibitors and centrifuged at 350g for 5 minutes at 4ºC to remove cellular
166 debris. Protein concentrations were determined in the supernatant using BCA™ protein assay kit.
167 Supernatant was centrifuged at 15,000g for 30 minutes at 4ºC and the new supernatant contained
168 soluble globular actin (G-actin). The insoluble filamentous actin (F-actin) in the pellet was then
169 resuspended and incubated on ice for 1 hour in 250 µL F-actin depolymerization buffer, with gently
170 mixing every 15 minutes. Samples were centrifuged at 15,000g for 30 minutes at 4ºC and this
171 supernatant was used to measure F-actin content by western blot. Twenty µL of the G-actin
172 fraction and 40 µL of the F-actin fractions were loaded and analyzed by western blot.

173

174

175 **Adeno-associated viruses**

176 AAV2-Rac1-DN-GFP (AAV-Rac1-DN; $3.5x10^{12}$ vg/ml) was produced by the Duke Viral Vector
177 Core (Durham, North Carolina). The plasmid containing the T17N Rac1 mutation (plasmid
178 #22784, pCyPet-Rac1(T17N)) and AAV-GFP (pAAV.CMV.PI.EGFP.WPRE.bGH; $1.6x10^{13}$ vg/ml)
179 were purchased from Addgene. AAV-GFP was diluted to match the concentration of AAV-Rac1-
180 DN.

181

182 **Confirmation of AAV-Rac1-DN in cells**

183 HEK293 cells were plated at 120,000 cells per well on a 12-well-plate. The media was changed
184 to 1% FBS-DMEM 24 hours prior to the infection. The cells were then infected with 2 µL of AAV-
185 Rac1-DN virus ($3.5x10^{12}$ vg/ml). Seventy-two hours after the infection, cells were incubated with
186 10% FBS for 30 minutes. The cells were lysed and analyzed by western blot.

187

188 **Stereotaxic surgery**

189 Mice were anesthetized using vaporized isoflurane and were fixed in a stereotaxic frame (David
190 Kopf Instruments). To overexpress the virus in the entirety of the DMS, bilateral microinfusions
191 were accomplished using stainless steel injectors (33 gauge; Small Parts Incorporated)
192 connected to Hamilton syringes (10 µL, 1701) at two sites in the DMS (anteroposterior (AP) +1.1
193 mm, mediolateral (ML) ± 1.2 mm, dorsoventral (DV) -3 mm and AP +0.66 mm, ML ± 1.2 mm, DV
194 -2.8 mm measured from bregma). Animals received a 1µL bilateral infusion of AAV-GFP or AAV-
195 Rac1-DN-GFP ($3.5x10^{12}$ vg/ml) at an infusion rate of 0.1µL/min controlled by an automatic pump
196 (Harvard Apparatus). The injectors were left at the infusion site for 10 minutes after the conclusion
197 of the infusion to allow the virus to diffuse.

198 To image single neurons, a low-titer ($7x10^{9}$ - $3.5x10^{10}$ vg/ml) of AAV-GFP or AAV-Rac1-DN-GFP
199 was infused into the DMS (AP +1.1 mm, ML ± 1.2 mm, DV -2.8 mm). 0.5µL of each virus was

200 infused bilaterally at a rate of 0.1μL/min. Injectors were left in place for 10 minutes for viral
201 diffusion.
202
203 ***In vivo* confirmation of viral expression**
204 After the conclusion of an experiment, animals were euthanized by cervical dislocation and the
205 brains were removed. The brain was dissected on ice into 1-mm-thick coronal sections and green
206 fluorescent protein (GFP) was visualized and imaged using an EVOS FL tabletop fluorescent
207 microscope (ThermoFisher Scientific, Waltham, MA). Mice with surgeries that failed to elicit viral
208 overexpression were excluded from the study.
209
210 **Immunostaining**
211 Mice were euthanized by transcardial perfusion with 0.01M PBS followed by 4%
212 paraformaldehyde (PFA) in phosphate buffer, for 5 minutes each step. Brains were removed and
213 postfixed in 4% PFA for 24 hours before being transferred to a 30% sucrose solution for 3 days.
214 Brains were then frozen rapidly on dry ice before being coronally sectioned into 100 μm sections
215 using a Leica CM3050 cryostat (Leica Biosystems, Richmond, IL). Slices were placed in 0.01M
216 PBS and the ones containing the site of infection were selected to be stained. Sections were
217 blocked with 5% normal donkey serum for 4 hours. Slices were incubated in the primary antibody
218 over 48 hours at 4°C on an orbital shaker. After primary antibody incubation, slices were washed
219 3 times for 45 minutes each in PBS before secondary antibody incubation overnight at 4°C on an
220 orbital shaker. There was another cycle of washing before placing the slices onto Superfrost Plus
221 microscope slides (Fisher Scientific, Hampton, NH) and mounting slides using Prolong Gold
222 mounting medium (ThermoFisher Scientific, Waltham, MA). Slides were allowed 24 hours to dry
223 before the edges were sealed to prevent dehydration.
224
225

226 **Morphological analysis**

227 Low titer of AAV-GFP or AAV-Rac1-DN ($7x10^9$ - $3.5x10^{10}$ vg/ml) was infused bilaterally into the
228 DMS. After 1 week of recovery, mice underwent 7 weeks of IA20%2BC. Twenty-four hours after
229 the last drinking session, mice were euthanized, perfused, processed, and 100 µm coronal
230 sections were collected. Images of GFP-stained DMS neurons were acquired with a spinning disk
231 confocal microscope with a 40x objective and a Z-interval of 1µm (Nikon, Tokyo, Japan). Images
232 were deconvoluted using AutoQuantX (v3.1.3, Media cybernetics, Inc, Rockville, MD), and GFP
233 neurons were traced using Neurolucida software (MBF Biosciences, Williston, VT).

234 *Scholl analysis*: Dendritic branches were quantified using Sholl analysis (Sholl, 1953). Starting
235 radius of dendritic branches was 10µm and end radius was 160µm from the center of the soma
236 with an interval of 10µm between radii. Cell body area was measured using Fiji software (NIH).

237 *Spine Analysis:* Images of GFP-stained DMS neurons were acquired with a spinning disk confocal
238 microscope with a 100x objective and a Z-interval of 0.1µm (Nikon, Tokyo, Japan). Only distal
239 dendrites (3rd or 4th order) were analyzed. Morphological properties were analyzed using Imaris
240 software (Oxford Instruments, Concord, MA). Dendritic spines were classified based on a
241 combination of length and head and neck morphology. Spines were classified into four subtypes
242 as in (Laguesse et al., 2018): filipodia (>2µm length, indiscernible head), stubby (<1µm length, no
243 visible neck), mushroom (>0.4µm head width, short neck), thin (head width <0.4µm, long neck).

244

245 **Behavioral paradigms**

246 2-bottle choice drinking paradigm

247 *Intermittent access to 20% alcohol (IA20%2BC):* The paradigm was conducted as described in
248 (Laguesse et al., 2017). Mice were given 24-hour access to one bottle of 20% alcohol (v/v) in tap
249 water or one bottle of water. Drinking sessions started at 11:30AM Monday, Wednesday, and
250 Friday with 24- or 48-hour (weekend) withdrawal periods in between during which only water was
251 available. The bottles were alternated each session to prevent a side preference from developing.

252 The bottles were weighed at the end of each session and adjusted for spill. Mice were weighed
253 once a week. Animals that drank over 7g/kg/24hr were included in the study. See **Table 1** for
254 average values in each of the experiments. Percentile of alcohol preference (preference index)
255 was calculated by dividing the amount of alcohol drank to the amount of water+alcohol X100.
256 *Intermittent access to 1% sucrose:* Mice had access to a 2-bottle choice between water and 1%
257 sucrose three days a week for 24-hour periods for two weeks (Laguesse et al., 2017). Bottles
258 were weighed at the end of each session and switched in between. Between sessions, only water
259 was available. The bottle weights were spill-adjusted after each session. Mice were weighed
260 weekly, and 1% sucrose consumption was measured in milliliters per kilogram of bodyweight
261 (ml/kg). Food was available *ad libitum*.
262 *Continuous access to 10% alcohol:* Mice had access to a bottle of 10% alcohol (v/v) in tap water
263 and a bottle of water for 24 hours a day for 3 weeks (21 drinking sessions) (Laguesse et al., 2017)
264 Bottles were removed and weighed daily. Bottle positions were alternated to reduce side
265 preference development. The bottle weights were spill-adjusted after each session. Mice were
266 weighed weekly and alcohol consumption was calculated for each in grams per kilogram.
267 *Operant self-administration (OSA):* OSA was conducted as described in (Laguesse et al., 2017).
268 Mice underwent stereotaxic surgery and IA20%2BC for 7-8 weeks as described above. Prior to
269 training, animals were handled for 1-2 minutes per day for 3 consecutive days. OSA was
270 conducted during the dark phase of the reverse light/dark cycle in operant chambers (length: 22
271 cm, width: 20 cm, height: 14 cm). OSA boxes were connected to a computer running MED-PC to
272 control and record session activity. The operant chambers (Med-Associates; Georgia, VT) had
273 two levers (length: 1.5 cm, distance between: 11 cm, height above floor: 2.5 cm) on one wall. The
274 operant chambers were also equipped with a reward port between the levers (height above floor:
275 0.5 cm) that included a photo-beam to track port entries. Upon reward delivery, a 3-second tone
276 (2900Hz) and a cue-light above the reward port was activated. To receive a reward, the mouse
277 must press the active lever in a fixed-ratio 1 (FR1) schedule, where one active-lever press leads

278 to one reward. A successful completion of this condition resulted in a delivery of 10 μL of 20%
279 alcohol to the reward port. The mouse must enter the reward port twice to reactivate the active
280 lever, ensuring consumption of the reward. Animals received a total of 20 hours of training time
281 in the paradigm in the first week (two 6-hour and two 4-hour sessions) before transitioning to 2-
282 hour afternoon sessions that began consistently at 13:00. After 8 2-hour FR1 sessions, the
283 complexity of the task was increased to FR2, where two active lever presses were required for
284 one reward. Active lever presses, inactive lever presses, port entries, and reward deliveries were
285 measured. Consumption was normalized based on mouse body weight and rewards
286 administered. Discrimination index was calculated as the percentage of active lever presses
287 divided by total presses. The proportion of reward lever presses statistic was calculated by
288 comparing lever presses that led to a reward to total lever presses, including inactive lever
289 presses. Mice with low viral expression were excluded from the study.
290 *Sucrose operant self-administration*: OSA of 1% sucrose was slightly modified from conditions
291 described in (Laguesse et al., 2017). Specifically, mice underwent stereotaxic surgery to
292 overexpress AAV-GFP or AAV-Rac1-DN-GFP in the DMS. After allowing for viral overexpression,
293 mice began 1% sucrose self-administration training in the chambers previously described with
294 two 6-hour and two 4-hour training sessions in the first week. Animals were handled for 1-2
295 minutes daily for 3 consecutive days before training began. They then transitioned to 2-hour
296 afternoon sessions that began consistently at 13:00. After 8 2-hour FR1 sessions, the mice
297 transitioned to FR2. Mice with low viral expression were excluded from the study.
298
299 **Open-field test**
300 Mice infected with either AAV-GFP or AAV-Rac1-DN were placed in an open field (43cm x 43cm)
301 in low-light conditions and allowed to explore for 20 minutes (Warnault et al., 2016). Locomotor
302 activity was tracked using EthoVision XT software (Noldus, Leesburg, VA), and total movement
303 (cm) was reported.

304 **Data analysis**

305 GraphPad Prism 9 and MATLAB were used for statistical analysis.

306 *Biochemical analysis*: Data were analyzed using the appropriate statistical test, including one-
307 way ANOVA, two-way ANOVA, or two-tailed t-test for normal populations, or Kruskal-Wallis for
308 non-normal populations. *Post hoc* testing was done using Šidák's multiple comparisons test.
309 *Biochemical analysis*: Data were analyzed using the appropriate statistical test, including one-
310 way ANOVA, two-way ANOVA, or two-tailed t-test for normal populations, or Kruskal-Wallis for
311 non-normal populations. *Post hoc* testing was done using Šidák's multiple comparisons test.

312 IA20%2BC numbers are expressed as the mean ± SEM consumption over the final two weeks
313 (**Table 1**). Data was first tested for normality using the Shapiro-Wilk normality test with
314 accompanying QQ plot. Parametric tests were performed on data samples deemed to be derived
315 from normal populations. The results were determined to be statistically significant if the resulting
316 p-value was less than 0.05.

317 *Behavioral analysis*: IA-2BC and OSA data were analyzed using a two-way repeated-measures
318 ANOVA, followed by *post hoc* Šidák's multiple comparisons test. A two-tailed t-test was performed
319 on the open-field locomotion. The results were determined to be statistically significant if the
320 resulting p-value was less than 0.05.

321 **Results**

322 **Alcohol activates Rac1 in the DMS of male mice**

323 We first tested if repeated cycles of alcohol binge drinking and withdrawal activates Rac1
324 in the striatum of male mice. Specifically, animals were subjected to 7 weeks of 20% alcohol or
325 water choice for 24 hours a day, 3 days a week, with 24- or 48- (weekend) hour withdrawal periods
326 in between during which mice had access to water only. Mice consuming water for the same
327 duration were used as controls (**Figure 1A**). Striatal regions were dissected and harvested 4
328 hours after the beginning of a drinking session ("binge") or 24 hours after the end of a drinking
329 session ("withdrawal") (**Figure 1A**). Rac1-GTP pulldown assay was utilized to analyze the level
330 of active GTP-bound vs. inactive GDP-bound Rac1. We found that the activity of Rac1 was
331 unaltered by alcohol in the NAc (**Figure 1B, Table 1**) and the DLS (**Figure 1C, Table 1**) (NAc
332 Kruskal-Wallis test $H = 0.5731$, $p = 0.7761$; DLS One-way ANOVA: $F_{(2,15)} = 0.0139$, $p = 0.9862$).
333 In contrast, we discovered that 7 weeks IA20%2BC produced a robust activation of Rac1 in the
334 DMS during both binge and withdrawal (**Figure 1D, Table 1**) (One-way ANOVA: $F_{(2, 15)} = 8.233$,
335 $p = 0.0039$; *Post hoc*: Water vs. Binge $p = 0.0058$, W vs. WD $p = 0.0068$). The same pattern of
336 Rac1 activation was also observed during withdrawal after 4 weeks of IA20%2BC (**Extended**
337 **Figure 1A, Table 1**) (Unpaired t-test: $t_{(6)} = 2{,}938$, $p = 0.0260$). In contrast, Rac1 activity was
338 unaltered in the DMS of female mice undergoing 7 weeks of IA20%2BC (**Figure 1E, Table 1**)
339 (Kruskal-Wallis test $H = 0.2456$, $p = 0.8968$), suggesting that alcohol-dependent Rac1 activation
340 is sexually dimorphic. Together, these data suggest that chronic voluntary drinking of alcohol
341 produces a long-lasting activation of Rac1 in the DMS of male mice.

342

343 **Rac1 activation by alcohol in the DMS is specific**

344 Next, we set to determine the specificity of alcohol-dependent activation of Rac1 in the
345 DMS. The closely related small G-proteins RhoA and Cdc42 have also been linked with synaptic
346 and structural plasticity (Francis et al., 2019; Zhang et al., 2021). We found that levels of RhoA

347 and Cdc42 bound to GTP (**Figure 2A-B, Table 1**) were unchanged in the DMS at both binge and
348 withdrawal from IA20%2BC as compared to water-only drinking mice (RhoA One-way ANOVA:
349 $F_{(2, 15)} = 0.472$, $p = 0.06323$; Cdc42 Kruskal-Wallis test $H = 3.310$, $p = 0.1962$). To measure if
350 Rac1 is activated in response to moderate consumption of alcohol, we exposed mice to a 10%
351 continuous access (10%CA) 2-bottle-choice alcohol drinking paradigm in which mice were
352 allowed to choose between 10% alcohol and water continuously for 21 days, matching the number
353 IA20%2BC sessions. We detected no change in the activation of Rac1 in the DMS after 10%CA
354 (**Figure 2C, Table 1**) (Unpaired t-test: $t_{(10)} = 0.3960$, $p = 0.7004$), which implies that higher
355 concentration of alcohol and/or repeated cycles of binge and withdrawal are necessary for the
356 alcohol-dependent activation of Rac1 in the DMS.

357 To examine if Rac1 is activated in the DMS by a naturally rewarding substance, mice
358 underwent intermittent access to a 1% sucrose 2-bottle-choice paradigm for 2 weeks. We found
359 that Rac1 is not activated in the DMS of sucrose drinking mice (**Figure 2D, Table 1**) (Unpaired t-
360 test: $t_{(12)} = 0.5345$, $p = 0.6028$), suggesting that activation of Rac1 signaling in the DMS is specific
361 for alcohol and is not shared with natural reward. Together, these data suggest that the activation
362 of Rac1 in the DMS observed after chronic alcohol consumption is not generalized to other closely
363 related small G-proteins in the Rho family, is specific to repeated cycles of binge and withdrawal
364 of a 20% alcohol and is not shared with natural reward.

365

366 **Alcohol promotes LIM kinase activation and cofilin phosphorylation**

367 Rac1 activation leads to the downstream phosphorylation of LIMK which in turn
368 phosphorylates cofilin (Edwards et al., 1999). Therefore, we examined whether alcohol-mediated
369 Rac1 stimulation promotes the activation of LIMK and cofilin phosphorylation in the DMS. To test
370 this question, we measured the level of LIMK phosphorylation, and thus activation, as well as the
371 phosphorylation of cofilin in the DMS after 7 weeks of IA20%2BC. We found that the
372 phosphorylation of both LIMK and cofilin were significantly increased after alcohol binge and

373 withdrawal in comparison to animals that drank water only (**Figure 3A-B, Table 1**) (One-way
374 ANOVA: LIMK $F_{(2, 12)} = 96.40$, $p < 0.0001$; *Post hoc*: Water vs. Binge $p < 0.0001$, Water vs.
375 Withdrawal $p < 0.0001$; Cofilin $F_{(2, 12)} = 44.14$, $p < 0.0001$; *Post hoc*: Water vs. Binge $p < 0.0001$,
376 Water vs. Withdrawal $p < 0.0001$). Together, these data suggest that the long-term alcohol
377 consumption activates Rac1-dependent signaling.
378
379 **Alcohol activation of the LIMK/cofilin signaling pathway in the DMS depends on Rac1**
380 The LIMK/cofilin signaling pathway can also be activated by other small G-proteins such
381 as RhoA/B, Cdc42, and Rac3 (Edwards et al., 1999; Mira et al., 2000; Swanson et al., 2017).
382 Thus, to confirm that the upregulation of LIMK and cofilin phosphorylation after excessive alcohol
383 use is indeed due to the increase in Rac1 activity, we used a dominant negative Rac1 mutant to
384 inhibit the activity of the endogenous protein. Specifically, the dominant negative mutant of Rac1
385 (Rac1-DN) contains a threonine to asparagine substitution at residue 17 (Worthylake et al., 2000).
386 The Rac1 mutant forms a tight complex with Rac1-specific GEFs, but does not allow the exchange
387 of GDP to GTP, keeping the G-protein constantly inactive (Ridley et al., 1992; Wong et al., 2006;
388 Zhang et al., 2016) (**Figure 4A**). Rac1-DN was packaged into an adeno-associated virus (AAV).
389 First, to confirm the inhibitory action of Rac1-DN, HEK293 cells were infected with AAV-Rac1-DN
390 in media containing 1% serum (**Extended Figure 2A**). Next, cells were incubated for 30 minutes
391 with media containing 10% FBS. As shown in **Extended Figure 2C**, incubation of cells with 10%
392 FBS increased LIMK phosphorylation in non-infected cells, which was not observed in cells
393 infected with AAV-Rac1-DN. In contrast, ERK1/2 whose phosphorylation does not depend on
394 Rac1 was increased by 10% serum in both uninfected cells and AAV-Rac1-DN infected cells.
395 These data suggest that AAV-Rac1-DN selectively inhibits Rac1 signaling in cultured cells.
396 Next, mice were bilaterally infected with AAV-Rac1-DN (3.5×10^{12} vg/ml) or an AAV-GFP
397 (3.5×10^{12} vg/ml) control in the DMS. As shown in **Figure 4B** and **Extended Figure 2E-F,** intense
398 and localized infection was detected in mice infected with AAV-Rac1-DN. Global Rac1 protein

399 level was significantly increased in the DMS of mice infected with AAV-Rac1-DN compared to
400 mice infected with AAV-GFP in mice drinking water or alcohol (**Extended Figure 2G**) (Two-way
401 ANOVA: Effect of virus $F_{(1,20)}$ = 69.58, p<0.0001; Effect of alcohol $F_{(1,20)}$ = 6.774, p = 0.0170;
402 Effect of virus x alcohol $F_{(1,20)}$ = 0.2164, p = 0.6468; *Post hoc* W+AAV-GFP vs. W+AAV-Rac1-
403 DN p<0.0001; A+AAV-GFP vs. A+AAV-Rac1-DN p = 0.0001).

404 We then tested if Rac1 is required for alcohol-mediated LIMK and cofilin phosphorylation
405 in the DMS. Three weeks after surgery, mice underwent 7 weeks of IA20%2BC before dissection
406 (**Figure 4C**). As described below, infection of the DMS of mice with AAV-GFP and AAV-Rac1-DN
407 did not alter alcohol consumption (**Figure 8B**), thus the DMS of mice infected with AAV-GFP or
408 AAV-Rac1-DN were exposed to the same concentration of alcohol (**Table 1**). The phosphorylation
409 of LIMK and cofilin were measured in the DMS of water- or alcohol-drinking mice infected with
410 AAV-GFP or AAV-Rac1-DN. We observed a significant increase in the phosphorylation of LIMK
411 and cofilin in AAV-GFP-infected animals during alcohol withdrawal (**Figure 4D-E, Table 1**) (Two-
412 way ANOVA: pLIMK Effect of alcohol $F_{(1,20)}$ = 35.12, p<0.0001; *Post hoc*: Water+AAV-GFP vs.
413 Alcohol+AAV-GFP p<0.0001; pCofilin Effect of alcohol $F_{(1,20)}$ = 380.5, p<0.0001; *Post hoc:*
414 Water+AAV-GFP vs. Alcohol+AAV-GFP p<0.0001), which aligns with our prior results (**Figure**
415 **3A-B**). AAV-Rac1-DN overexpression had no effect on the phosphorylation of LIMK or cofilin in
416 water-drinking animals (Two-way ANOVA: pLIMK Effect of virus $F_{(1,20)}$ = 58.01, p<0.0001; *Post*
417 *hoc*: Water+AAV-GFP vs. Water+AAV-Rac1-DN p = 0.3184; pCofilin Effect of virus $F_{(1,20)}$ = 378.8,
418 p<0.0001; *Post hoc:* Water+AAV-GFP vs. Water+AAV-Rac1-DN p = 0.9679). In contrast,
419 overexpression of AAV-Rac1-DN significantly reduced alcohol-mediated phosphorylation of LIMK
420 and cofilin (Two-way ANOVA: pLIMK Effect of virus x alcohol $F_{(1,20)}$ = 105.1, p<0.0001; *Post hoc*:
421 Alcohol+AAV-GFP vs. Alcohol+AAV-Rac1-DN p<0.0001; pCofilin Effect of virus x alcohol $F_{(1,20)}$ =
422 423.8, p<0.0001; *Post hoc:* Alcohol+AAV-GFP vs. Alcohol+AAV-Rac1-DN p<0.0001). These
423 results suggest that the molecular consequences of Rac1 stimulation by alcohol in the DMS is

424 the phosphorylation, and therefore activation, of LIMK and the phosphorylation of its substrate
425 cofilin.
426
427 **Alcohol promotes F-actin formation in the DMS via Rac1**
428 We previously showed that chronic excessive alcohol intake increases F-actin assembly
429 and decreases G-actin in the DMS (Laguesse et al., 2018). Phosphorylated cofilin is unable to
430 cleave F-actin into G-actin (Bamburg, 1999). Therefore, we hypothesized that the consequence
431 of the alcohol-mediated activation of the Rac1/LIMK/cofilin signaling is the formation of F-actin.
432 To determine if actin remodeling in the DMS depends on Rac1 signaling, we examined the level
433 of F-actin and G-actin in the DMS of mice that underwent 7 weeks of IA20%2BC or water and
434 that were infected with AAV-GFP or AAV-Rac1-DN (**Figure 5A, Table 1**). Similar to previous
435 findings (Laguesse et al., 2018), control mice infected with AAV-GFP in the DMS had a
436 significantly higher level of F-actin after excessive chronic alcohol consumption in comparison to
437 AAV-GFP-infected mice that drank water only (Two-way ANOVA: Effect of alcohol $F_{(1,20)} = 101.6$,
438 $p<0.0001$; *Post hoc*: Water+AAV-GFP vs. Alcohol+AAV-GFP $p<0.0001$). Conversely, mice
439 infected with AAV-Rac1-DN had a significantly lower F-actin content in comparison to AAV-GFP
440 mice both in the water- and alcohol-consuming groups (Two-way ANOVA: Effect of virus $F_{(1,20)} =$
441 105.4, $p<0.0001$; *Post hoc*: Water+AAV-GFP vs. Water+AAV-Rac1-DN $p = 0.0199$; Alcohol+AAV-
442 GFP vs. Alcohol+AAV-Rac1-DN $p<0.0001$). In addition, the magnitude of the difference in F-actin
443 levels is greater between alcohol-drinking AAV-GFP and AAV-Rac1-DN mice compared to water-
444 only animals (**Figure 5B, Table 1**) (Two-way ANOVA: Effect of virus x alcohol $F_{(1,20)} = 30.92$,
445 $p<0.0001$). Overexpression of AAV-Rac1-DN had no effect on the level of G-actin in the water-
446 only group. However, G-actin levels were reduced by alcohol in mice infected with AAV-GFP,
447 which was rescued by overexpression of AAV-Rac1-DN (**Figure 5B, Table 1**) (Two-way ANOVA:
448 Effect of virus $F_{(1,20)} = 7.585$, $p = 0.0122$; Effect of alcohol $F_{(1,20)} = 12.30$, $p = 0.0022$; Effect of virus
449 x alcohol $F_{(1,20)} = 11.73$, $p = 0.0027$; *Post hoc*: Water+AAV-GFP vs. Alcohol+AAV-GFP $p = 0.0005$;

450 Water+AAV-Rac1-DN vs. Alcohol+AAV-GFP p = 0.0016; Alcohol+AAV-GFP vs. Alcohol+AAV-
451 Rac1-DN p = 0.0018). Therefore, these data suggest that the alcohol-mediated increase in F-
452 actin assembly in the DMS depends on Rac1.
453
454 **Rac1 promotes the remodeling of dendritic arbors in the DMS**
455 F-actin is responsible for morphological remodeling in neurons (Honkura et al., 2008;
456 Chazeau and Giannone, 2016; Costa et al., 2020). Previously, we showed that alcohol
457 consumption increases dendritic branch complexity in DMS medium spiny neurons (MSNs)
458 (Wang et al., 2015; Laguesse et al., 2018). Since alcohol reduces F-actin content via Rac1, we
459 hypothesized that the increase in dendritic branching after alcohol use is mediated via Rac1
460 signaling. To test this possibility, the DMS of mice that were subjected to IA20%2BC or water only
461 was infected with a low titer ($7x10^9$ - $3.5x10^{10}$ vg/ml) of AAV-Rac1-DN or AAV-GFP. The goal was
462 to infect a sparse population of neurons to allow for imaging of individual arbors (**Figure 6A-C**).
463 Low-titer infection of Rac1-DN did not alter alcohol consumption (**Table 1**). Sholl analysis (Sholl,
464 1953) was then performed on the DMS of water- or alcohol-drinking mice infected with AAV-GFP
465 or AAV-Rac1-DN.
466 Similar to our prior findings (Wang et al., 2015; Laguesse et al., 2018), we found that
467 alcohol significantly increased the complexity of dendritic trees of DMS MSNs (Three-way
468 ANOVA: Effect of alcohol x distance $F_{(1,1008)} = 7.132$, $p < 0.0001$). Specifically, DMS dendrites 30-
469 90µm from the soma exhibited significantly more intersections in alcohol-drinking vs. water-only-
470 drinking mice (**Figure 6D**) (Two-way ANOVA: Effect of alcohol $F_{(1, 65)} = 17.24$, $p < 0.0001$, *Post*
471 *hoc Šídák's multiple comparisons test*). The increase in dendritic complexity was further quantified
472 by calculating the area under the curve (AUC) (**Figure 6E**) (Two-way ANOVA: Effect of alcohol
473 $F_{(1, 63)} = 15.24$, $p = 0.0002$). In addition, we observed that dendritic length (**Figure 6F**), the number
474 of branching points (**Figure 6G**), and the number of ending points (**Figure 6H**), were also
475 significantly increased by alcohol (Two-way ANOVA: Effect of alcohol Dendritic Length $F_{(1, 63)}$ =

476 16.92, $p < 0.0001$; Branching points $F_{(1, 63)} = 9.086$, $p = 0.0037$; Ending points $F_{(1, 63)} = 11.48$, $p =$
477 0.0016).

478 In contrast, infection of the DMS with AAV-Rac1-DN significantly reduced dendritic
479 arborization (Three-way ANOVA: Effect of virus x distance $F_{(1,1008)} = 6.462$, $p < 0.0001$).
480 Specifically, the number of dendritic intersections 20-80μm from the soma was significantly
481 decreased when DMS neurons were infected with AAV-Rac1-DN as compared to neurons
482 infected with AAV-GFP (**Figure 6D**) (Two-way ANOVA of consolidated data: Effect of virus $F_{(1, 65)}$
483 $= 15.59$, $p = 0.0002$, *Post hoc Šídák's multiple comparisons test of each Sholl diameter,*
484 *represented graphically*). Furthermore, AAV-Rac1-DN infection decreased AUC (**Figure 6E**),
485 along with dendritic length, branching points, and ending points (**Figure 6F-H**) (Two-way ANOVA:
486 Effect of virus AUC $F_{(1, 63)} = 13.17$, $p = 0.0006$, Dendritic length $F_{(1, 63)} = 14.88$, $p = 0.0002$,
487 Branching points $F_{(1, 63)} = 11.94$, $p = 0.0010$, Ending points $F_{(1, 63)} = 16.35$, $p = 0.0002$). However,
488 there was no interaction between the variables (Three-way ANOVA: Effect of alcohol x virus x
489 distance $F_{(1,1008)} = 0.4689$, $p = 0.9617$; Two-way ANOVA: Effect of alcohol x virus AUC $F_{(1,63)} =$
490 0.04500, $p = 0.8327$, Dendritic length $F_{(1,63)} = 0.01739$, $p = 0.8955$, Branching points $F_{(1,63)} =$
491 0.03059, $p = 0.8617$, Ending points $F_{(1,63)} = 0.2592$, $p = 0.6125$).

492 Next, we examined the number of branches per dendritic order (**Figure 6I**). Three-way
493 ANOVA showed a significant main effect of virus ($F_{(1,63)} = 13.21$, $p = 0.0006$) and a significant main
494 effect of alcohol ($F_{(1,63)} = 11.31$, $p = 0.0013$) but no interaction between virus and alcohol ($F_{(1,63)} =$
495 0.5889, $p = 0.4457$). The number of branches was then analyzed for each order and two-way
496 ANOVA showed a significant main effect of virus at 2nd, 3rd, and 5th order (represented
497 graphically), a significant main effect of alcohol at 3rd, 4th and 5th order.

498 Together, these data confirmed that chronic excessive alcohol use significantly increases
499 the complexity of dendritic branching in DMS MSNs (Wang et al., 2015; Laguesse et al., 2018).
500 Importantly, we show that Rac1 contributes to dendritic branching in DMS neurons.
501

502 **Rac1 in the DMS is required for the alcohol-mediated alteration in dendritic spine**
503 **morphology**

504 Actin is the major structural protein in the post-synaptic density (PSD) (Ratner and Mahler,
505 1983). Actin cytoskeleton organization directly controls dendritic spine morphology (Schubert and
506 Dotti, 2007; Hotulainen and Hoogenraad, 2010; Basu and Lamprecht, 2018). Rac1 signaling
507 controls actin dynamics and is involved in dendritic spine morphogenesis (Bosco et al., 2009;
508 Haditsch et al., 2009; Haditsch et al., 2013; Costa et al., 2020). Since Rac1 is activated by alcohol
509 which in turn promotes F-actin assembly we hypothesized that the dendritic spines in the DMS
510 are altered by alcohol in a Rac1-dependent manner.

511 Next, we examined the shape of individual dendritic spines on distal dendritic branches
512 (3rd or 4th order) in mice infected with AAV-GFP and AAV-Rac1DN in DMS and that consumed
513 20% alcohol or water only for 7 weeks (**Figure 7A**). Spine density (spine number per 10μm) was
514 unaffected by alcohol drinking or AAV-Rac1-DN infection (**Figure 7B**) (Two-way ANOVA: Effect
515 of virus $F_{(1,48)} = 0.7175$, $p = 0.4012$; Effect of alcohol $F_{(1,48)} = 2.541$, $p = 0.1175$; Effect of virus x
516 alcohol $F_{(1,48)} = 0.2495$, $p = 0.6197$).

517 We found that in control mice infected with AAV-GFP, alcohol drinking significantly
518 increased dendritic spine area, aligning with prior findings (Laguesse et al., 2018) (Two-way
519 ANOVA: Effect of alcohol $F_{(1,48)} = 36.24$, $p < 0.0001$) (**Figure 7C**). Alcohol drinking also
520 significantly increased dendritic spine volume (Two-way ANOVA: Effect of alcohol $F_{(1,48)} = 32.76$,
521 $p < 0.0001$) (**Figure 7D**). While spine length was unaffected by alcohol drinking (**Figure 7E**),
522 average spine head width was increased (**Figure 7F**) (Two-way ANOVA: Spine Length Effect of
523 alcohol $F_{(1,48)} = 0.9881$, $p = 0.5408$; Head Width Effect of alcohol $F_{(1,48)} = 18.81$, $p < 0.0001$), which
524 led to a reduction in length-to-width ratio by alcohol (**Figure 7G**) (Two-way ANOVA: Effect of
525 alcohol $F_{(1,48)} = 5.490$, $p = 0.0233$).

526 In contrast, the alcohol-mediated alterations in dendritic spine morphology were
527 attenuated by Rac1 inhibition. Specifically, Rac1 inhibition significantly decreased dendritic spine

528 area in alcohol-drinking animals, without affecting water-only controls. (**Figure 7C)** (Two-way
529 ANOVA: Effect of virus $F_{(1,48)}$ = 12.98, p = 0.0007; Effect of virus x alcohol $F_{(1,48)}$ = 12.52, p =
530 0.0021; *Post hoc Šídák's multiple comparisons test*). The alcohol-mediated increase in dendritic
531 spine volume was also prevented by Rac1-DN, without affecting water-only controls (**Figure 7D**)
532 (Two-way ANOVA: Effect of virus $F_{(1,48)}$ = 8.552, p = 0.0053; Effect of virus x alcohol $F_{(1,48)}$ = 9.659,
533 p = 0.0032; *Post hoc Šídák's multiple comparisons test*). In addition, we found that AAV-Rac1-
534 DN slightly reduced spine length independent of drinking (**Figure 7E**), and prevented the alcohol-
535 mediated increase in spine head width (**Figure 7F**) (Two-way ANOVA: Spine Length Effect of
536 virus $F_{(1,48)}$ = 4.610, p = 0.0369; Effect of virus x alcohol $F_{(1,48)}$ = 0.4081, p = 0.5260; Head Width
537 Effect of virus $F_{(1,48)}$ = 3.408, p = 0.0710; Effect of virus x alcohol $F_{(1,48)}$ = 6.734, p = 0.0125; *Post*
538 *hoc Šídák's multiple comparisons test*). Finally, length-to-width ratio was unaffected by AAV-
539 Rac1-DN infection (**Figure 7G**) (Two-way ANOVA: Effect of virus $F_{(1,48)}$ = 0.5552, p = 0.4598;
540 Effect of virus x alcohol $F_{(1,48)}$ = 1.939, p = 0.1701; *Post hoc Šídák's multiple comparisons test)*.
541 Together, these findings suggest that Rac1 contributes to the alcohol-mediated increases in
542 dendritic spine area, volume, and spine head width.

543 We then examined whether alcohol-mediated activation of Rac1 signaling and the
544 increase in F-actin content was responsible for the maturation of DMS MSN dendritic spines.
545 Dendritic spines are classed into four subtypes: filipodia, thin, stubby, and mushroom, with
546 filopodia being the least mature form of spines and mushrooms being the most mature form (Kasai
547 et al., 2003). Spines are characterized by different shape, with primary variables being spine
548 length, neck, and head width (Kasai et al., 2003). Like our previous study (Laguesse et al., 2018),
549 we found that alcohol drinking increased the maturity of dendritic spines in the DMS. Specifically,
550 we found that in AAV-GFP infected mice, alcohol significantly increased the proportion of
551 mushroom-shaped spines at the expense of thin spines, while not affecting filopodia or stubby
552 spines (**Figure 7H**). Rac1 inhibition blocked the alcohol-mediated increase in mushroom spines
553 and decrease in thin spines but had no effect on animals drinking water only (**Figure 7H**) (Three-

554 way ANOVA: Effect of virus $F_{(1, 48)} = 0.9904$, $p = 0.3246$; Effect of alcohol $F_{(1, 48)} = 0.9904$, $p =$
555 0.3246; Spine type $F_{(3, 144)} = 358.0$, $p < 0.0001$; Effect of virus x spine type $F_{(3, 144)} = 14.80$, $p <$
556 0.0001; Effect of alcohol x spine type $F_{(3, 144)} = 11.12$, $p < 0.0001$, Effect of virus x alcohol x spine
557 type $F_{(3, 144)} = 14.23$, $p < 0.0001$; *Post hoc Šídák's multiple comparisons test*). Together, our data
558 suggest that Rac1 signaling is responsible for the alcohol-mediated morphological changes in
559 dendritic spine structure and maturation in DMS MSNs.
560
561 **Rac1 does not play a role in the development and maintenance of voluntary alcohol intake**
562 Next, we set to determine if the alcohol-dependent, Rac1-mediated molecular and cellular
563 changes have consequences on alcohol-related behaviors. First, we tested the effect of Rac1
564 inhibition on the development of excessive alcohol drinking. To do so, the DMS of mice was
565 bilaterally infused with AAV-Rac1-DN or AAV-GFP ($3.5x10^{12}$ vg/ml). After allowing for three weeks
566 of recovery, animals underwent IA20%2BC for 7 weeks and drinking and preference were
567 measured (**Figure 8A**). We found that there was no difference in alcohol consumption in the group
568 with overexpressed AAV-Rac1-DN in the DMS compared to AAV-GFP controls (**Figure 8B**) (RM
569 Two-way ANOVA: Effect of virus $F_{(1,17)} = 0.08351$, $p = 0.7761$; Effect of session $F_{(6, 102)} = 5.420$, p
570 < 0.0001; Effect of virus x session $F_{(6, 102)} = 0.1339$, $p = 0.9916$), and alcohol preference was also
571 unaltered (**Figure 8C**) (RM Two-way ANOVA: Effect of virus $F_{(1,17)} = 0.1798$, $p = 0.6768$; Effect of
572 session $F_{(6, 102)} = 3.196$, $p = 0.0065$; Effect of virus x session $F_{(6, 102)} = 0.4250$, $p = 0.8608$).
573 Next, we determined the potential contribution of Rac1 to the maintenance of alcohol-
574 drinking behavior. Mice were first subjected to the IA20%2BC paradigm for 7 weeks. Experimental
575 and control groups were balanced based on drinking average. IA20%2BC was then resumed for
576 4 weeks (**Figure 8D**). Overexpression of AAV-Rac1-DN did not alter the maintenance of alcohol
577 drinking (**Figure 8E**) (RM Two-way ANOVA: Effect of virus $F_{(1,14)} = 2.454$, $p = 0.1396$; Effect of
578 session $F_{(3,42)} = 1.262$, $p = 0.2998$; Effect of virus x session $F_{(3,42)} = 0.5923$, $p = 0.6235$) or alcohol

579 preference (**Figure 8F**) (RM Two-way ANOVA: Effect of virus $F_{(1, 14)} = 2.520$, $p = 0.1347$; Effect
580 of session $F_{(3,42)} = 0.7839$, $p = 0.5096$; Effect of virus x session $F_{(3,42)} = 0.7518$, $p = 0.5275$).
581 Overexpression of AAV-Rac1-DN did not alter water consumption in the development
582 (**Supp. Figure 3A**) or maintenance (**Supp. Figure 3B**) drinking experiments (RM Two-way
583 ANOVA: Development Effect of virus $F_{(1,17)} = 0.4571$, $p = 0.5081$; Effect of session $F_{(6,102)} = 3.855$,
584 $p = 0.0017$; Effect of virus x session $F_{(6,102)} = 0.8631$, $p = 0.5248$; Maintenance Effect of virus $F_{(1,13)}$
585 $= 0.8287$, $p = 0.3792$; Effect of session $F_{(3, 39)} = 3.606$, $p = 0.0216$; Effect of virus x session $F_{(3,39)}$
586 $= 0.1149$, $p = 0.9508$) Together, these results suggest that Rac1 in the DMS does not contribute
587 to the development or maintenance of voluntary alcohol drinking in the IA20%2BC paradigm.
588
589 **Rac1 in the DMS is required for alcohol-associated goal-directed learning**
590 We observed that the activation of Rac1 signaling after chronic excessive alcohol use was
591 specific to the DMS, a brain region that is associated with goal-directed learning (Dolan and
592 Dayan, 2013; Shan et al., 2014). As goal-directed behavior is particularly important for drug
593 seeking (Singer et al., 2018), we hypothesized that Rac1 in the DMS may play a role in alcohol-
594 associated goal-directed learning.
595 To examine this hypothesis, the DMS of mice was bilaterally infused with AAV-Rac1-DN
596 or AAV-GFP ($3.5x10^{12}$ vg/ml). Mice were allowed 3 weeks to recover before undergoing
597 IA20%2BC for 7 weeks. Mice were then trained to self-administer 20% alcohol on a fixed ratio of
598 reinforcement 1 (FR1) schedule for 20 hours over four sessions during the first week before
599 transitioning to 2-hour sessions. After eight 2-hour sessions of FR1, mice progressed to FR2, and
600 alcohol-associated active lever presses and inactive lever presses were examined (**Figure 9A**).
601 We found that there was no significant change in active lever presses between mice infected with
602 AAV-Rac1-DN or AAV-GFP (**Figure 9B, Table 1**) (RM Two-way ANOVA: Effect of virus $F_{(13, 143)}$
603 $= 1.522$, $p = 0.1163$; Effect of session $F_{(3.043, 33.47)} = 1.232$, $p = 0.3137$; Effect of virus x session
604 $F_{(13, 143)} = 1.522$, $p = 0.1163$). However, mice infected with AAV-Rac1-DN pressed the inactive

605 lever significantly more than the AAV-GFP-infected mice (**Figure 9C**) (RM Two-way ANOVA:
606 Effect of virus $F_{(1, 11)} = 5.102$, $p = 0.0452$; Effect of session $F_{(13, 143)} = 0.9024$, $p = 0.5522$; Effect of
607 virus x session $F_{(13, 143)} = 0.8569$, $p = 0.5996$). This phenotype is exemplified in the discrimination
608 index, showing that the AAV-Rac1-DN mice exhibited significantly worse discrimination for the
609 active lever throughout the OSA experiment in comparison to AAV-GFP controls (**Figure 9D**) (RM
610 Two-way ANOVA: Effect of virus $F_{(1, 11)} = 5.320$, $p = 0.0415$; Effect of session $F_{(13, 143)} = 2.237$, p
611 = 0.0107; Effect of virus x session $F_{(13,143)} = 0.8674$, $p = 0.5886$). A similar phenotype was
612 observed in the proportion of rewarded lever presses, which accounts for active lever presses
613 that do not lead to a reward. Specifically, while over 50% of presses of the AAV-GFP control
614 animals led to a reward, the AAV-Rac1-DN group failed to reach this threshold throughout the
615 testing period (**Figure 9E**) (RM Two-way ANOVA: Effect of virus $F_{(1,11)} = 16.66$, $p = 0.0018$, Effect
616 of session $F_{(13,143)} = 6.400$, $p < 0.0001$; Effect of virus x session $F_{(13,143)} = 0.5518$, $p = 0.8880$).
617 There was no difference in alcohol consumption between groups (**Figure 9F**) (RM Two-way
618 ANOVA: Effect of virus $F_{(1,11)} = 1.099$, $p = 0.3169$; Effect of session $F_{(13, 143)} = 15.18$, $p < 0.0001$;
619 Effect of virus x session $F_{(13, 143)} = 1.156$, $p = 0.3178$), which aligns with the IA20%2BC data
620 (**Figure 7B, 7E**). Examination of the inter-response interval between lever presses of the final
621 session shows that AAV-Rac1-DN mice exhibited a significantly increased proportion of lever
622 presses in short intervals, and significantly less lever presses in the longer intervals, compared to
623 AAV-GFP controls (**Figure 9G**) (RM Two-way ANOVA: Effect of virus $F_{(1,11)} = 0.5360$, $p = 0.4794$;
624 Effect of interval $F_{(4,44)} = 64.48$, $p < 0.0001$; Effect of virus x interval $F_{(4, 44)} = 6.145$, $p = 0.0005$;
625 *Post hoc* 0-5 $p = 0.0034$, >20 $p < 0.001$). These phenotypes can be visualized in the behavioral
626 trace of individual mouse profiles from the OSA session with the greatest discrimination difference
627 (**Figure 9H**). These data suggest that Rac1 in the DMS plays a role in alcohol-associated, goal-
628 directed learning. As the DMS plays an important role in movement (Kravitz and Kreitzer, 2012),
629 we examined the consequence of Rac1 inhibition in the DMS on locomotion using an open field

630 paradigm. As shown in **Figure 9I**, attenuation of Rac1 activity in the DMS had no effect on
631 locomotion (Unpaired t-test: $t_{(16)}$ = 0.06783, p = 0.9468).
632
633 **Rac1 in the DMS is not required for sucrose goal-directed learning**
634 Alcohol is often distinct from natural reward (Alhadeff et al., 2019; Nall et al., 2021; Martins
635 et al., 2022), and Rac1 in the DMS is not activated in response to sucrose consumption (**Figure**
636 **2D**). We hypothesized that Rac1 in the DMS does not play a role in sucrose-dependent goal
637 directed learning. To test this hypothesis, the DMS of mice was first bilaterally infused with AAV-
638 Rac1-DN or AAV-GFP ($3.5x10^{12}$ vg/ml) and age-matched to the alcohol OSA group. The mice
639 were then trained to operant self-administer 1% sucrose, initially starting with an FR1
640 reinforcement schedule for 20 hours of training over four sessions before transitioning to 2-hour
641 sessions. After 8 2-hour sessions of FR1, mice were advanced to an FR2 schedule (**Figure 10A**).
642 We observed no difference between mice with AAV-Rac1-DN and AAV-GFP overexpression in
643 active lever pressing (**Figure 10B**), inactive lever pressing (**Figure 10C**), discrimination (**Figure**
644 **10D**), or proportion of rewarded lever presses (**Figure 10E**) (RM Two-way ANOVA: **10B** Effect of
645 virus $F_{(1,11)}$ = 4.651, p = 0.0540; Effect of session $F_{(3.905, 42.36)}$ = 5.335, p = 0.0015; Effect of virus x
646 session $F_{(13,141)}$ = 0.9458, p = 0.5079; **10C** Effect of virus $F_{(1,11)}$ = 0.2087, p = 0.6566; Effect of
647 session $F_{(2.224, 24.12)}$ = 0.8833, p = 0.4364; Effect of virus x session $F_{(13,141)}$ = 0.6457, p = 0.8119;
648 **10D** Effect of virus $F_{(1,11)}$ = 0.007081, p = 0.9344; Effect of session $F_{(3.161, 34.29)}$ = 1.888, p = 0.1475;
649 Effect of virus x session $F_{(13,141)}$ = 0.7552, p = 0.7057; **10E** Effect of virus $F_{(1,11)}$ = 0.0001974, p =
650 0.9890; Effect of session $F_{(3.512, 38.10)}$ = 6.534, p = 0.0007; Effect of virus x session $F_{(13,141)}$ = 0.7314,
651 p = 0.7298). These data suggest that Rac1 in the DMS does not affect learning of natural-reward-
652 associated goal-directed behavior and that the learning deficiency exhibited by AAV-Rac1-DN
653 overexpression in the DMS is specific to alcohol-associated goal-directed learning.
654
655

656 **Discussion**

657 We show herein that Rac1 signaling is activated in the DMS in response to long term
658 excessive alcohol drinking of male mice. We further show that the consequences of alcohol-
659 mediated Rac1/LIMK signaling in the DMS are the formation of F-actin and the alteration of
660 dendritic spine morphology. Finally, we present data to suggest that Rac1 in the DMS plays a role
661 in alcohol-associated goal-directed learning. Together, our results suggest that Rac1 in the DMS
662 plays an important role in molecular and morphological adaptations that promote alcohol-
663 dependent learning behavior.

664

665 **Rac1 is activated in the DMS after alcohol consumption**

666 We found that Rac1 signaling is activated specifically in the DMS of male mice in response
667 to long-term drinking of alcohol which was observed during the 4-hour binge drinking session and
668 was still detected after 24 hours of withdrawal. The mechanism by which alcohol activates Rac1
669 in the DMS is unknown, and the sequence of events is unclear, e.g. is the binge or withdrawal
670 session that initiates the activation of Rac1? Rac1 is activated by NMDA receptor stimulation in
671 rat cortical and hippocampal neurons (Tolias et al., 2005; Xiao et al., 2013). Previously, we found
672 that *ex vivo* and *in vivo* exposure to, and withdrawal from, alcohol induces long-term facilitation of
673 GluN2B-containing NMDA receptor activity specifically in the DMS (Wang et al., 2007; Wang et
674 al., 2010). Glutamatergic tone is increased in cortical regions that project to the striatum of
675 humans and rats during acute alcohol withdrawal (Hermann et al., 2012; Hwa et al., 2017).
676 Therefore, it is very plausible that Rac1 is first activated during withdrawal through the activation
677 of GluN2B receptors in the DMS, and that its activity is maintained during the alcohol drinking
678 session. The long-lasting activation of Rac1 in the DMS in response to alcohol could be due to
679 increased level and/or activity of one or both of its specific GEFs, Tiam1 and/or Karilin-7 (Tolias
680 et al., 2005; Xie et al., 2007) or because of a reduction of the level and/or activity of its specific
681 GAP (Toure et al., 1998; Garcia-Mata et al., 2006; Peru et al., 2012; Nakamura, 2013). Another

682 plausible explanation for alcohol-mediated Rac1 activation in the DMS is that withdrawal from
683 IA20%2BC might trigger activation of a DMS-specific circuit by activating only neurons projecting
684 to the DMS. For example, Ma et al. found an increase in glutamatergic transmission from mPFC
685 neurons projecting to the DMS in alcohol but not water drinking rats (Ma et al., 2017). In addition,
686 chronic IA20%2BC drinking was shown to alter instrumental learning by affecting the thalamus-
687 to-DMS circuit (Ma et al., 2022). Further work is required to unravel the specificity of inputs and
688 its interaction with alcohol.

689 Furthermore, ~95% of the DMS MSNs express either dopamine D1 receptor- (D1) or
690 dopamine D2 receptor (Gerfen and Surmeier, 2011; Calabresi et al., 2014; Cheng et al., 2017).
691 Alcohol increases the complexity of dendritic branching and maturation of dendritic spines
692 selectively in D1 but not D2 DMS MSNs (Wang et al., 2015). Since the inhibition of endogenous
693 Rac1 attenuates alcohol-dependent re-structuring of DMS MSNs, we speculate that alcohol-
694 mediated Rac1 signaling is specifically localized to D1 neurons. This possibility will be determined
695 in future studies.

696 Interestingly, we did not detect Rac1 activation in response to alcohol drinking in the DMS
697 of female mice. While Rac1 is not activated in the DMS of female mice in response to alcohol
698 drinking, this does not exclude Rac1 from being activated by alcohol in other brain regions, such
699 as the amygdala or hippocampus, where Rac1 is involved in learning and memory (Martinez et
700 al., 2007; Haditsch et al., 2009; Wu et al., 2014; Gao et al., 2015). Further investigation is required
701 to unravel the mechanisms controlling sex-specificity in Rac1 signaling.

702

703 **Rac1 in the DMS promotes alcohol-dependent morphological adaptations**

704 We previously showed that the complexity of dendritic branching is increased by alcohol
705 (Wang et al., 2015; Laguesse et al., 2018). Here, we replicated the data of both studies and
706 showed that Rac1 is responsible for DMS MSNs dendritic complexity. However, because Rac1-
707 DN significantly decreased dendritic arborization in both water and alcohol drinking animals, we

708 cannot definitely conclude that Rac1 contributes to alcohol-dependent alteration of dendritic tree
709 complexity, but based on the finding that Rac1 inhibition significantly alters F-actin content, this
710 possibility is highly likely.

711 Rac1 is involved in the maturation and morphogenesis of dendritic spines (Nakayama et
712 al., 2000; Tashiro et al., 2000; Pennucci et al., 2019; Costa et al., 2020). In addition to the DMS,
713 (Wang et al., 2015; Laguesse et al., 2018) and data herein, alcohol exposure affects dendritic
714 spine morphology in cortical regions such as the medial prefrontal cortex (mPFC) (Cannady et
715 al., 2021), and the OFC (McGuier et al., 2015). Therefore, it is plausible that the activation of Rac1
716 may also be the molecular mediator of alcohol-dependent structural plasticity in cortical regions.

717 Interestingly, Rac1 was reported to play a role in cocaine-dependent neuroadaptations in
718 other striatal regions. Specifically, Dietz et al. reported that cocaine-dependent increase in NAc
719 thin spine density was mediated by Rac1 (Dietz et al., 2012), whereas Li et al. showed that the
720 cocaine-dependent increase of Rac1 signaling in the dorsal striatum leads to dendritic spine
721 maturation (Li et al., 2015). Cocaine also increases actin cycling through LIMK/cofilin signaling in
722 the NAc (Toda et al., 2006). Tu et al. observed that decreased Rac1 signaling is required for
723 METH-mediated spine density and maturation in the NAc (Tu et al., 2019). Here, the increase in
724 dendritic maturation after alcohol drinking in the DMS is shown to be Rac1-dependent. These
725 findings suggest that drugs of abuse are altering Rac1 signaling in a drug- and subregion-
726 dependent manner.

727

728 **Rac1 and alcohol-associated behaviors**

729 We found that Rac1 in the DMS does not play a role in voluntary drinking behavior. It is
730 not unusual that alcohol-mediated signaling controls a specific behavior without affecting
731 voluntary drinking. For example, inhibition of mTORC1 activity in the orbitofrontal cortex (OFC)
732 attenuates habitual alcohol seeking without affecting IA20%2BC consumption (Morisot et al.,
733 2019). Furthermore, lack of toll-like receptor 4 (TLR4) does not alter ethanol consumption or

734 preference (Blednov et al., 2017a), but does significantly reduce the duration of loss of righting
735 reflex and recovery from alcohol-induced motor incoordination (Blednov et al., 2017b). Although
736 Rac1 signaling in the DMS does not mediate voluntary drinking behavior, its activation may be
737 involved in other alcohol-related behaviors.

738 The DMS primarily mediates goal-directed behaviors (Yin et al., 2005; Balleine and
739 O'Doherty, 2010; Everitt and Robbins, 2013; Gremel and Costa, 2013), which play a major role
740 in the addiction cycle (Hogarth, 2020). Here, Rac1 inhibition in the DMS impaired active lever
741 discrimination and led to a reduction in the proportion of lever presses leading to a reward,
742 implying a failure to learn the association between an active lever press and alcohol reward. The
743 increase in inactive lever presses is unlikely to have resulted from increased locomotor activity,
744 as Rac1 inhibition did not affect locomotion. Interestingly, this learning deficit is specific for
745 alcohol, as Rac1 inhibition in the DMS did not affect the learning of active lever association with
746 sucrose reward. This phenotype could be the result of disrupting the Rac1 signaling reinforcing
747 active lever preference ("GO") or the avoidance of undesired action ("No-GO") (Cheng et al.,
748 2017). The normal physiological role of Rac1 in the DMS is unknown. Rac1 has been linked with
749 learning and memory in other regions such as the hippocampus, where it is required for spatial
750 learning (Haditsch et al., 2009). Rac1 in the hippocampus also mediates reversible forgetting (Lv
751 et al., 2019), contributing to the long-term maintenance of memory behaviors like contextual-fear
752 conditioning and object recognition (Lv et al., 2019). Further work is required to investigate Rac1's
753 role in goal-directed behavior.

754 To our knowledge, this is the first study unveiling a molecular mechanism involved in
755 alcohol-specific goal-directed learning. Prior studies have investigated the mechanisms of goal-
756 directed learning in the context of food and sucrose seeking in the rodent striatum (Hart et al.,
757 2018; Matamales et al., 2020; Peak et al., 2020). For example, using chemogenetics, Peak et al.
758 found that D1R MSNs in the posterior DMS were critical for sucrose goal-directed learning (Peak
759 et al., 2020), and Matamales et al. have shown that striatal-dependent goal-directed learning for

760 food involves ensembles of D1R MSNs, controlled and modified by D2R MSNs (Matamales et al.,
761 2020). It is tempting to speculate that specific sucrose or alcohol ensembles exist within the DMS.
762 With Rac1 signaling contributing to alcohol but not sucrose self-administration, our results provide
763 support to the notion that natural reward and alcohol drug reward mechanisms are different
764 (Alhadeff et al., 2019).

765 In summary, in this study we unraveled that alcohol drinking increases Rac1 signaling in
766 the DMS, leading to the alcohol-mediated maturation of dendritic spines, which is important for
767 the goal-directed behavior learning process. As goal-directed behavior is a major contributor to
768 the cycle of addiction (Hogarth, 2020), it is likely that the maladaptive activation of Rac1
769 contributes to the progression of AUD.

770 **Author Contributions:** DR conceived the project. ZWH, YE, and DR designed the

771 experiments. ZWH, KP, AS, SL and YE conducted the experiments and analyzed the data. CS

772 provided technical support. ZWH, YE, and DR wrote the manuscript.

773

774 **References**

775 Alhadeff AL, Goldstein N, Park O, Klima ML, Vargas A, Betley JN (2019) Natural and Drug
776 Rewards Engage Distinct Pathways that Converge on Coordinated Hypothalamic and Reward
777 Circuits. Neuron 103:891-908 e896.

778 Andrianantoandro E, Pollard TD (2006) Mechanism of actin filament turnover by severing and
779 nucleation at different concentrations of ADF/cofilin. Mol Cell 24:13-23.

780 Balleine BW, O'Doherty JP (2010) Human and rodent homologies in action control: corticostriatal
781 determinants of goal-directed and habitual action. Neuropsychopharmacology 35:48-69.

782 Bamburg JR (1999) Proteins of the ADF/cofilin family: essential regulators of actin dynamics.
783 Annu Rev Cell Dev Biol 15:185-230.

784 Basu S, Lamprecht R (2018) The Role of Actin Cytoskeleton in Dendritic Spines in the
785 Maintenance of Long-Term Memory. Front Mol Neurosci 11:143.

786 Bernard O (2007) Lim kinases, regulators of actin dynamics. Int J Biochem Cell Biol 39:1071-
787 1076.

788 Blednov YA, Black M, Chernis J, Da Costa A, Mayfield J, Harris RA (2017a) Ethanol Consumption
789 in Mice Lacking CD14, TLR2, TLR4, or MyD88. Alcohol Clin Exp Res 41:516-530.

790 Blednov YA, Black M, Benavidez JM, Da Costa A, Mayfield J, Harris RA (2017b) Sedative and
791 Motor Incoordination Effects of Ethanol in Mice Lacking CD14, TLR2, TLR4, or MyD88. Alcohol
792 Clin Exp Res 41:531-540.

793 Bokoch GM (2003) Biology of the p21-activated kinases. Annu Rev Biochem 72:743-781.

794 Bosco EE, Mulloy JC, Zheng Y (2009) Rac1 GTPase: a "Rac" of all trades. Cell Mol Life Sci
795 66:370-374.

796 Calabresi P, Picconi B, Tozzi A, Ghiglieri V, Di Filippo M (2014) Direct and indirect pathways of
797 basal ganglia: a critical reappraisal. Nat Neurosci 17:1022-1030.

798 Cannady R, Nguyen T, Padula AE, Rinker JA, Lopez MF, Becker HC, Woodward JJ, Mulholland
799 PJ (2021) Interaction of chronic intermittent ethanol and repeated stress on structural and
800 functional plasticity in the mouse medial prefrontal cortex. Neuropharmacology 182:108396.
801 Chazeau A, Giannone G (2016) Organization and dynamics of the actin cytoskeleton during
802 dendritic spine morphological remodeling. Cell Mol Life Sci 73:3053-3073.
803 Cheng Y, Huang CCY, Ma T, Wei X, Wang X, Lu J, Wang J (2017) Distinct Synaptic Strengthening
804 of the Striatal Direct and Indirect Pathways Drives Alcohol Consumption. Biol Psychiatry 81:918-
805 929.
806 Chin SM, Jansen S, Goode BL (2016) TIRF microscopy analysis of human Cof1, Cof2, and ADF
807 effects on actin filament severing and turnover. J Mol Biol 428:1604-1616.
808 Corbetta S, Gualdoni S, Ciceri G, Monari M, Zuccaro E, Tybulewicz VL, de Curtis I (2009)
809 Essential role of Rac1 and Rac3 GTPases in neuronal development. FASEB J 23:1347-1357.
810 Costa JF, Dines M, Lamprecht R (2020) The Role of Rac GTPase in Dendritic Spine
811 Morphogenesis and Memory. Front Synaptic Neurosci 12:12.
812 Dietz DM et al. (2012) Rac1 is essential in cocaine-induced structural plasticity of nucleus
813 accumbens neurons. Nat Neurosci 15:891-896.
814 Dolan RJ, Dayan P (2013) Goals and habits in the brain. Neuron 80:312-325.
815 Edwards DC, Sanders LC, Bokoch GM, Gill GN (1999) Activation of LIM-kinase by Pak1 couples
816 Rac/Cdc42 GTPase signalling to actin cytoskeletal dynamics. Nat Cell Biol 1:253-259.
817 Everitt BJ, Robbins TW (2013) From the ventral to the dorsal striatum: devolving views of their
818 roles in drug addiction. Neurosci Biobehav Rev 37:1946-1954.
819 Francis TC, Gaynor A, Chandra R, Fox ME, Lobo MK (2019) The Selective RhoA Inhibitor Rhosin
820 Promotes Stress Resiliency Through Enhancing D1-Medium Spiny Neuron Plasticity and
821 Reducing Hyperexcitability. Biol Psychiatry 85:1001-1010.

822 Gao Q, Yao W, Wang J, Yang T, Liu C, Tao Y, Chen Y, Liu X, Ma L (2015) Post-training activation
823 of Rac1 in the basolateral amygdala is required for the formation of both short-term and long-term
824 auditory fear memory. Front Mol Neurosci 8:65.
825 Garcia-Mata R, Wennerberg K, Arthur WT, Noren NK, Ellerbroek SM, Burridge K (2006) Analysis
826 of activated GAPs and GEFs in cell lysates. Methods Enzymol 406:425-437.
827 Gerfen CR, Surmeier DJ (2011) Modulation of striatal projection systems by dopamine. Annu Rev
828 Neurosci 34:441-466.
829 Golden SA, Christoffel DJ, Heshmati M, Hodes GE, Magida J, Davis K, Cahill ME, Dias C, Ribeiro
830 E, Ables JL, Kennedy PJ, Robison AJ, Gonzalez-Maeso J, Neve RL, Turecki G, Ghose S,
831 Tamminga CA, Russo SJ (2013) Epigenetic regulation of RAC1 induces synaptic remodeling in
832 stress disorders and depression. Nat Med 19:337-344.
833 Gremel CM, Costa RM (2013) Orbitofrontal and striatal circuits dynamically encode the shift
834 between goal-directed and habitual actions. Nat Commun 4:2264.
835 Haditsch U, Anderson MP, Freewoman J, Cord B, Babu H, Brakebusch C, Palmer TD (2013)
836 Neuronal Rac1 is required for learning-evoked neurogenesis. J Neurosci 33:12229-12241.
837 Haditsch U, Leone DP, Farinelli M, Chrostek-Grashoff A, Brakebusch C, Mansuy IM, McConnell
838 SK, Palmer TD (2009) A central role for the small GTPase Rac1 in hippocampal plasticity and
839 spatial learning and memory. Mol Cell Neurosci 41:409-419.
840 Hart G, Bradfield LA, Balleine BW (2018) Prefrontal Corticostriatal Disconnection Blocks the
841 Acquisition of Goal-Directed Action. J Neurosci 38:1311-1322.
842 Hermann D, Weber-Fahr W, Sartorius A, Hoerst M, Frischknecht U, Tunc-Skarka N, Perreau-
843 Lenz S, Hansson AC, Krumm B, Kiefer F, Spanagel R, Mann K, Ende G, Sommer WH (2012)
844 Translational magnetic resonance spectroscopy reveals excessive central glutamate levels
845 during alcohol withdrawal in humans and rats. Biol Psychiatry 71:1015-1021.
846 Hogarth L (2020) Addiction is driven by excessive goal-directed drug choice under negative affect:
847 translational critique of habit and compulsion theory. Neuropsychopharmacology 45:720-735.

848 Honkura N, Matsuzaki M, Noguchi J, Ellis-Davies GC, Kasai H (2008) The subspine organization
849 of actin fibers regulates the structure and plasticity of dendritic spines. Neuron 57:719-729.
850 Hotulainen P, Hoogenraad CC (2010) Actin in dendritic spines: connecting dynamics to function.
851 J Cell Biol 189:619-629.
852 Hwa L, Besheer J, Kash T (2017) Glutamate plasticity woven through the progression to alcohol
853 use disorder: a multi-circuit perspective. F1000Res 6:298.
854 Kanellos G, Frame MC (2016) Cellular functions of the ADF/cofilin family at a glance. Journal of
855 Cell Science 129:3211-3218.
856 Kasai H, Matsuzaki M, Noguchi J, Yasumatsu N, Nakahara H (2003) Structure-stability-function
857 relationships of dendritic spines. Trends Neurosci 26:360-368.
858 Koob G, Kreek MJ (2007) Stress, dysregulation of drug reward pathways, and the transition to
859 drug dependence. Am J Psychiatry 164:1149-1159.
860 Kravitz AV, Kreitzer AC (2012) Striatal mechanisms underlying movement, reinforcement, and
861 punishment. Physiology (Bethesda) 27:167-177.
862 Laguesse S, Morisot N, Phamluong K, Sakhai SA, Ron D (2018) mTORC2 in the dorsomedial
863 striatum of mice contributes to alcohol-dependent F-Actin polymerization, structural modifications,
864 and consumption. Neuropsychopharmacology 43:1539-1547.
865 Laguesse S, Morisot N, Shin JH, Liu F, Adrover MF, Sakhai SA, Lopez MF, Phamluong K, Griffin
866 WC, 3rd, Becker HC, Bender KJ, Alvarez VA, Ron D (2017) Prosapip1-Dependent Synaptic
867 Adaptations in the Nucleus Accumbens Drive Alcohol Intake, Seeking, and Reward. Neuron
868 96:145-159 e148.
869 Li J, Zhang L, Chen Z, Xie M, Huang L, Xue J, Liu Y, Liu N, Guo F, Zheng Y, Kong J, Zhang L,
870 Zhang L (2015) Cocaine activates Rac1 to control structural and behavioral plasticity in caudate
871 putamen. Neurobiol Dis 75:159-176.
872 Lv L, Liu Y, Xie J, Wu Y, Zhao J, Li Q, Zhong Y (2019) Interplay between alpha2-chimaerin and
873 Rac1 activity determines dynamic maintenance of long-term memory. Nat Commun 10(1):5313.

874 Ma T, Barbee B, Wang X, Wang J (2017) Alcohol induces input-specific aberrant synaptic
875 plasticity in the rat dorsomedial striatum. Neuropharmacology 123:46-54.
876 Ma T, Huang Z, Xie X, Cheng Y, Zhuang X, Childs MJ, Gangal H, Wang X, Smith LN, Smith RJ,
877 Zhou Y, Wang J (2022) Chronic alcohol drinking persistently suppresses thalamostriatal excitation
878 of cholinergic neurons to impair cognitive flexibility. J Clin Invest 132(4):e154969.
879 Maciver SK, Hussey PJ (2002) The ADF/cofilin family: actin-remodeling proteins. Genome Biol
880 3(5):reviews3007.
881 Martinez LA, Klann E, Tejada-Simon MV (2007) Translocation and activation of Rac in the
882 hippocampus during associative contextual fear learning. Neurobiol Learn Mem 88:104-113.
883 Martins JS, Joyner KJ, McCarthy DM, Morris DH, Patrick CJ, Bartholow BD (2022) Differential
884 brain responses to alcohol-related and natural rewards are associated with alcohol use and
885 problems: Evidence for reward dysregulation. Addict Biol 27:e13118.
886 Matamales M, McGovern AE, Mi JD, Mazzone SB, Balleine BW, Bertran-Gonzalez J (2020) Local
887 D2- to D1-neuron transmodulation updates goal-directed learning in the striatum. Science
888 367:549-555.
889 McGuier NS, Padula AE, Lopez MF, Woodward JJ, Mulholland PJ (2015) Withdrawal from chronic
890 intermittent alcohol exposure increases dendritic spine density in the lateral orbitofrontal cortex of
891 mice. Alcohol 49:21-27.
892 Mira JP, Benard V, Groffen J, Sanders LC, Knaus UG (2000) Endogenous, hyperactive Rac3
893 controls proliferation of breast cancer cells by a p21-activated kinase-dependent pathway. Proc
894 Natl Acad Sci U S A 97:185-189.
895 Morisot N, Phamluong K, Ehinger Y, Berger AL, Moffat JJ, Ron D (2019) mTORC1 in the
896 orbitofrontal cortex promotes habitual alcohol seeking. Elife 8:e51333.
897 Nakamura F (2013) FilGAP and its close relatives: a mediator of Rho-Rac antagonism that
898 regulates cell morphology and migration. Biochem J 453:17-25.

899 Nakayama AY, Harms MB, Luo L (2000) Small GTPases Rac and Rho in the maintenance of
900 dendritic spines and branches in hippocampal pyramidal neurons. J Neurosci 20:5329-5338.
901 Nall RW, Heinsbroek JA, Nentwig TB, Kalivas PW, Bobadilla AC (2021) Circuit selectivity in drug
902 versus natural reward seeking behaviors. J Neurochem 157:1450-1472.
903 Nguyen LK, Kholodenko BN, von Kriegsheim A (2018) Rac1 and RhoA: Networks, loops and
904 bistability. Small GTPases 9:316-321.
905 Pavlov D, Muhlrad A, Cooper J, Wear M, Reisler E (2007) Actin filament severing by cofilin. J Mol
906 Biol 365:1350-1358.
907 Peak J, Chieng B, Hart G, Balleine BW (2020) Striatal direct and indirect pathway neurons
908 differentially control the encoding and updating of goal-directed learning. Elife 9:e58544.
909 Pennucci R, Gucciardi I, de Curtis I (2019) Rac1 and Rac3 GTPases differently influence the
910 morphological maturation of dendritic spines in hippocampal neurons. PLoS One 14:e0220496.
911 Peru YCdPRL, Acevedo SF, Rodan AR, Chang LY, Eaton BA, Rothenfluh A (2012) Adult neuronal
912 Arf6 controls ethanol-induced behavior with Arfaptin downstream of Rac1 and RhoGAP18B. J
913 Neurosci 32:17706-17713.
914 Ratner N, Mahler HR (1983) Structural organization of filamentous proteins in postsynaptic
915 density. Biochemistry 22:2446-2453.
916 Reijnders MRF et al. (2017) RAC1 Missense Mutations in Developmental Disorders with Diverse
917 Phenotypes. Am J Hum Genet 101:466-477.
918 Ridley AJ (2006) Rho GTPases and actin dynamics in membrane protrusions and vesicle
919 trafficking. Trends Cell Biol 16:522-529.
920 Ridley AJ, Paterson HF, Johnston CL, Diekmann D, Hall A (1992) The small GTP-binding protein
921 rac regulates growth factor-induced membrane ruffling. Cell 70:401-410.
922 Schubert V, Dotti CG (2007) Transmitting on actin: synaptic control of dendritic architecture. J
923 Cell Sci 120:205-212.

924 Scott RW, Olson MF (2007) LIM kinases: function, regulation and association with human
925 disease. J Mol Med (Berl) 85:555-568.
926 Shan Q, Ge M, Christie MJ, Balleine BW (2014) The acquisition of goal-directed actions generates
927 opposing plasticity in direct and indirect pathways in dorsomedial striatum. J Neurosci 34:9196-
928 9201.
929 Sholl DA (1953) Dendritic organization in the neurons of the visual and motor cortices of the cat.
930 J Anat 87:387-406.
931 Singer BF, Fadanelli M, Kawa AB, Robinson TE (2018) Are Cocaine-Seeking "Habits" Necessary
932 for the Development of Addiction-Like Behavior in Rats? J Neurosci 38:60-73.
933 Swanson AM, DePoy LM, Gourley SL (2017) Inhibiting Rho kinase promotes goal-directed
934 decision making and blocks habitual responding for cocaine. Nat Commun 8:1861.
935 Tashiro A, Minden A, Yuste R (2000) Regulation of dendritic spine morphology by the rho family
936 of small GTPases: antagonistic roles of Rac and Rho. Cereb Cortex 10:927-938.
937 Tejada-Simon MV (2015) Modulation of actin dynamics by Rac1 to target cognitive function. J
938 Neurochem 133:767-779.
939 Toda S, Shen HW, Peters J, Cagle S, Kalivas PW (2006) Cocaine increases actin cycling: effects
940 in the reinstatement model of drug seeking. J Neurosci 26:1579-1587.
941 Tolias KF, Bikoff JB, Burette A, Paradis S, Harrar D, Tavazoie S, Weinberg RJ, Greenberg ME
942 (2005) The Rac1-GEF Tiam1 couples the NMDA receptor to the activity-dependent development
943 of dendritic arbors and spines. Neuron 45:525-538.
944 Toure A, Dorseuil O, Morin L, Timmons P, Jegou B, Reibel L, Gacon G (1998) MgcRacGAP, a
945 new human GTPase-activating protein for Rac and Cdc42 similar to Drosophila rotundRacGAP
946 gene product, is expressed in male germ cells. J Biol Chem 273:6019-6023.
947 Tu G, Ying L, Ye L, Zhao J, Liu N, Li J, Liu Y, Zhu M, Wu Y, Xiao B, Guo H, Guo F, Wang H,
948 Zhang L, Zhang L (2019) Dopamine D(1) and D(2) Receptors Differentially Regulate Rac1 and

949 Cdc42 Signaling in the Nucleus Accumbens to Modulate Behavioral and Structural Plasticity After
950 Repeated Methamphetamine Treatment. Biol Psychiatry 86:820-835.
951 Van Aelst L, D'Souza-Schorey C (1997) Rho GTPases and signaling networks. Genes Dev
952 11:2295-2322.
953 Vetter IR, Wittinghofer A (2001) The guanine nucleotide-binding switch in three dimensions.
954 Science 294:1299-1304.
955 Wang J, Lanfranco MF, Gibb SL, Yowell QV, Carnicella S, Ron D (2010) Long-lasting adaptations
956 of the NR2B-containing NMDA receptors in the dorsomedial striatum play a crucial role in alcohol
957 consumption and relapse. J Neurosci 30:10187-10198.
958 Wang J, Cheng Y, Wang X, Roltsch Hellard E, Ma T, Gil H, Ben Hamida S, Ron D (2015) Alcohol
959 Elicits Functional and Structural Plasticity Selectively in Dopamine D1 Receptor-Expressing
960 Neurons of the Dorsomedial Striatum. J Neurosci 35:11634-11643.
961 Wang J, Carnicella S, Phamluong K, Jeanblanc J, Ronesi JA, Chaudhri N, Janak PH, Lovinger
962 DM, Ron D (2007) Ethanol induces long-term facilitation of NR2B-NMDA receptor activity in the
963 dorsal striatum: implications for alcohol drinking behavior. J Neurosci 27:3593-3602.
964 Wang W, Ju YY, Zhou QX, Tang JX, Li M, Zhang L, Kang S, Chen ZG, Wang YJ, Ji H, Ding YQ,
965 Xu L, Liu JG (2017) The Small GTPase Rac1 Contributes to Extinction of Aversive Memories of
966 Drug Withdrawal by Facilitating GABA(A) Receptor Endocytosis in the vmPFC. J Neurosci
967 37:7096-7110.
968 Wang X, Liu D, Wei F, Li Y, Wang X, Li L, Wang G, Zhang S, Zhang L (2020) Stress-Sensitive
969 Protein Rac1 and Its Involvement in Neurodevelopmental Disorders. Neural Plast 2020:8894372.
970 Warnault V, Darcq E, Morisot N, Phamluong K, Wilbrecht L, Massa SM, Longo FM, Ron D (2016)
971 The BDNF Valine 68 to Methionine Polymorphism Increases Compulsive Alcohol Drinking in Mice
972 That Is Reversed by Tropomyosin Receptor Kinase B Activation. Biol Psychiatry 79:463-473.
973 Wong KW, Mohammadi S, Isberg RR (2006) Disruption of RhoGDI and RhoA regulation by a
974 Rac1 specificity switch mutant. J Biol Chem 281:40379-40388.

975 Worthylake DK, Rossman KL, Sondek J (2000) Crystal structure of Rac1 in complex with the
976 guanine nucleotide exchange region of Tiam1. Nature 408:682-688.
977 Wu P, Ding ZB, Meng SQ, Shen HW, Sun SC, Luo YX, Liu JF, Lu L, Zhu WL, Shi J (2014)
978 Differential role of Rac in the basolateral amygdala and cornu ammonis 1 in the reconsolidation
979 of auditory and contextual Pavlovian fear memory in rats. Psychopharmacology (Berl) 231:2909-
980 2919.
981 Xiao L, Hu C, Yang W, Guo D, Li C, Shen W, Liu X, Aijun H, Dan W, He C (2013) NMDA receptor
982 couples Rac1-GEF Tiam1 to direct oligodendrocyte precursor cell migration. Glia 61:2078-2099.
983 Xie Z, Srivastava DP, Photowala H, Kai L, Cahill ME, Woolfrey KM, Shum CY, Surmeier DJ,
984 Penzes P (2007) Kalirin-7 controls activity-dependent structural and functional plasticity of
985 dendritic spines. Neuron 56:640-656.
986 Yang N, Higuchi O, Ohashi K, Nagata K, Wada A, Kangawa K, Nishida E, Mizuno K (1998) Cofilin
987 phosphorylation by LIM-kinase 1 and its role in Rac-mediated actin reorganization. Nature
988 393:809-812.
989 Yin HH, Ostlund SB, Knowlton BJ, Balleine BW (2005) The role of the dorsomedial striatum in
990 instrumental conditioning. Eur J Neurosci 22:513-523.
991 Zhang C, Liu J, Zhao Y, Yue X, Zhu Y, Wang X, Wu H, Blanco F, Li S, Bhanot G, Haffty BG, Hu
992 W, Feng Z (2016) Glutaminase 2 is a novel negative regulator of small GTPase Rac1 and
993 mediates p53 function in suppressing metastasis. Elife 5:e10727.
994 Zhang H, Ben Zablah Y, Zhang H, Jia Z (2021) Rho Signaling in Synaptic Plasticity, Memory, and
995 Brain Disorders. Front Cell Dev Biol 9:729076.

996 **Table 1. Average Alcohol Consumption for biochemical experiments**

Figure	Average Consumption (g/kg/24hr)	SEM (±g/kg/24hr)
1B NAc	13.38	1.025
1C DLS	13.38	1.060
1D DMS	14.53	0.982
1E Female DMS	19.59	0.979
2A RhoA	12.31	0.4461
2B Cdc42	13.67	0.7354
2C 10%CA	8.787	0.2611
3A-B pLIMK pCofilin	15.34	0.5169
4D-E;5B AAV-GFP	14.00	0.7264
4D-E;5B AAV-Rac1-DN	13.68	0.4589
6, 7 AAV-GFP	10.63	0.5058
6, 7 AAV-Rac1-DN	10.88	1.223
9 AAV-GFP	12.10	0.7463
9 AAV-Rac1-DN	12.36	1.046
Supp. 1A 4wk DMS	12.560	1.678
2D Sucrose	174.81 (ml/kg)	17.87 (ml/kg)

997 **Figure 1. Alcohol activates Rac1 in the DMS of male mice**

998 **(A)** Intermittent access to 20% alcohol in 2-bottle-choice (IA20%2BC) experimental timeline. **(B-**
999 **D)** The NAc **(B)**, the DLS **(C)**, and the DMS **(D)** were harvested 4 hours into last drinking session
1000 (binge, B) or after 24 hours of abstinence (withdrawal, WD). Rac1-GTP pull-down assay was
1001 conducted on cell lysates. Levels of GTP-bound Rac1 were normalized to total Rac1 and
1002 presented as percentage of the average of the water values. **(E)** Female mice underwent
1003 IA20%2BC before the DMS was harvested and the percentage of Rac1-GTP was calculated.
1004 Data are represented as mean ± SEM and analyzed using one-way ANOVA (C, D) with *post hoc*
1005 Šidák's multiple comparisons test, or Kruskal-Wallis test for non-parametric distributions (B, E).
1006 *$p < 0.05$, **$p<0.01$, ***$p < 0.001$; ns, non-significant. n = 6 per group.

1007

1008 **Figure 2. Rac1 activation by alcohol in the DMS is specific**

1009 **(A-B)** Mice underwent IA20%2BC as described in Figure 1A, and the DMS was harvested 4 hours
1010 into the last drinking session (binge, B) or after 24 hours of abstinence (withdrawal, WD). RhoA-
1011 GTP **(A)** or Cdc42-GTP **(B)** pull-down assay was conducted on cell lysates and quantified using
1012 western blot. Levels of GTP-bound RhoA or Cdc42 were normalized to total respective protein
1013 and presented as percentage of average of the water values. **(C)** Mice underwent 21 sessions of
1014 10%CA and the DMS was harvested. Rac1-GTP pull-down assay was conducted on cell lysates
1015 and quantified using western blot. Rac1-GTP was normalized to total Rac1 and presented as
1016 percentage of average of water values. **(D)** Mice underwent intermittent access to 1% sucrose for
1017 2 weeks and the DMS was harvested. Rac1-GTP pull-down assay was performed on cell lysates,
1018 and Rac1-GTP was normalized to total Rac1 and presented as average of water values. Data are
1019 represented as mean ± SEM and analyzed using one-way ANOVA (A), Kruskal-Wallis test (B), or
1020 unpaired two-tailed t-test (C, D). ns, non-significant. n = 6-7 per group.

1021

1022

1023 **Figure 3. Alcohol promotes LIM Kinase activation and cofilin phosphorylation**

1024 **(A-B)** Mice underwent 7 weeks of IA20%2BC as in Figure 1A, and LIMK and cofilin
1025 phosphorylation in the DMS were examined using western blot analysis. The levels of phospho-
1026 LIMK (pLIMK) and phospho-Cofilin (pCofilin) were normalized to total respective protein and
1027 quantified as a percentage of the average of the water values. All data are represented as
1028 mean ± SEM and analyzed by one-way ANOVA with *post hoc* Šidák's multiple comparisons test.
1029 ***$p < 0.001$. n = 5 per group.

1030

1031 **Figure 4. Alcohol activation of the LIMK/cofilin signaling pathway in the DMS depends on**
1032 **Rac1**

1033 **(A)** Rac1-DN mechanism of action. Rac1-DN has a mutation in its P-loop and does not bind GTP.
1034 GEFs bind to Rac1-DN but are unable to exchange GDP for GTP. The GEFs remain bound to
1035 Rac1-DN and ignore endogenous Rac1. **(B)** Confirmation of viral overexpression during
1036 dissection on the DMS of a mouse infected with AAV-Rac1-DN. 2X image from EVOS FL tabletop
1037 fluorescent microscope. **(C)** Experimental timeline. Mice received bilateral infusion of AAV-Rac1-
1038 DN or AAV-GFP in the DMS and were allowed 3 weeks for overexpression. After IA20%2BC or
1039 water only for 7 weeks the DMS was harvested. **(C-D)** Phosphorylation of LIMK and cofilin were
1040 examined using western blot analysis. Levels of pLIMK and pCofilin were normalized to total
1041 respective protein and quantified as a percentage of AAV-GFP-infected, water-only animals. Data
1042 are represented as mean ± SEM and analyzed by two-way ANOVA with *post hoc* Šidák's multiple
1043 comparisons test. *$p<0.05$, ****$p<0.0001$; ns, non-significant. n = 6 per group.

1044

1045 **Figure 5. Alcohol promotes F-actin formation in the DMS via Rac1**

1046 **(A)** Experimental timeline. Mice received a bilateral infusion of AAV-Rac1-DN or AAV-GFP in the
1047 DMS and were allowed 3 weeks for overexpression. Mice underwent IA20%2BC or water-only
1048 drinking for 7 weeks before the DMS was harvested. **(B)** G-actin/F-actin assay was conducted on

1049 the DMS of mice after overexpression surgery and IA20%2BC or water-only drinking. The
1050 filamentous (F) or globular (G) actin contents were examined using western blot analysis and
1051 normalized to total actin and quantified as a percentage of AAV-GFP-infected, water-only animals.
1052 Data represented as mean ± SEM and analyzed using two-way ANOVA with Šidák's multiple
1053 comparison. *p < 0.05, **p<0.01, ***p < 0.001, ****p<0.0001; ns, non-significant. n = 6 per group.
1054

1055 **Figure 6. Rac1 promotes remodeling of dendritic arbors in the DMS**

1056 Low titer of AAV-GFP or AAV-Rac1-DN ($7x10^9$ - $3.5x10^{10}$ vg/ml) was infused bilaterally into the
1057 DMS. After 1 week of recovery, mice underwent 7 weeks of IA20%2BC. Mice consuming water
1058 only were used as control. Twenty-four hours after the last drinking session, mice were perfused
1059 and brains were sliced into 100µm sections before MSN morphology was analyzed. **(A)** Sample
1060 image (40X magnification) of a GFP-positive DMS MSN. Scale bar, 50 µm. **(B)** Example of the
1061 reconstruction of the GFP-positive neuron. **(C)** Scheme of the morphological parameters
1062 measured in each neuron. Dendritic order increased after each branching point, defined as a
1063 dendritic intersection. **(D, E)** Analysis of neuronal dendritic arborization. Sholl analysis was
1064 performed on reconstructed neurons. The number of intersections was analyzed for each point
1065 **(D)** and the area under the curve (AUC) **(E)** was calculated. **(F)** Measurement of total dendritic
1066 length. **(G)** Number of branching points. **(H)** Number of ending points. **(I)** Number of branches per
1067 dendritic order. Data are represented as mean ± SEM and analyzed by two-way ANOVA. Main
1068 effect of virus is represented graphically. *p < 0.05, **p<0.01, ***p < 0.001. Water+AAV-GFP: 19
1069 neurons from 6 mice; Alcohol+AAV-GFP: 23 neurons from 7 mice; Water+AAV-Rac1-DN: 15
1070 neurons from 6 mice, Alcohol+AAV-Rac1-DN: 10 neurons from 3 mice.
1071
1072
1073

1074 **Figure 7. Rac1 in the DMS is required for the alcohol-mediated morphological changes in**
1075 **dendritic spines**
1076 Low titer of AAV-GFP or AAV-Rac1-DN ($7x10^9$ - $3.5x10^{10}$ vg/ml) was infused bilaterally into the
1077 DMS. After 1 week of recovery, mice underwent 7 weeks of IA20%-2BC. Mice consuming water
1078 only were used as control. Twenty-four hours after the last drinking session, mice were perfused,
1079 and MSN dendritic spine morphology was analyzed. **(A)** Sample image of a GFP-positive DMS
1080 MSN (100X magnification) from each group. Scale bar, 10 µm. **(B)** Average dendritic spine density
1081 (number of spines/10 µm). **(C)** Average dendritic spine area (μm^2). **(D)** Average dendritic spine
1082 volume (μm^3). **(E)** Average dendritic spine length (µm). **(F)** Average diameter of dendritic spine
1083 heads (µm). **(G)** Dendritic spine length-to-width ratio. Data is represented as mean ± SEM and
1084 analyzed using two-way ANOVA and Šidák's *post hoc* multiple comparisons test. *p<0.05,
1085 **p<0.01, ***p<0.001. ****p<0.0001. **(H)** Percentage of filopodia, thin, stubby, and mushroom
1086 dendritic spines for water- and alcohol-drinking mice infected with either AAV-GFP or AAV-Rac1-
1087 DN. Three-way ANOVA and Šidák's *post hoc* multiple comparisons test. ****p<0.0001.
1088 Water+AAV-GFP: 14 neurons from 5 mice; Alcohol+AAV-GFP: 13 neurons from 5 mice;
1089 Water+AAV-Rac1-DN: 14 neurons from 5 mice; Alcohol+AAV-Rac1-DN: 11 neurons from 4 mice.
1090

1091 **Figure 8. Rac1 does not play a role in the development and maintenance of voluntary**
1092 **alcohol intake**
1093 **(A)** Development: Surgery and IA20%2BC timeline. Mice received a bilateral, dual-infusion of
1094 AAV-Rac1-DN or AAV-GFP as a control. After 3 weeks of recovery, IA20%2BC began and
1095 continued for 7 weeks. **(B)** Weekly average alcohol consumption (g/kg/24hrs.) of development
1096 drinking mice. **(C)** Preference for alcohol during the development IA20%2BC drinking, with an
1097 index above 50 indicating a preference for alcohol. **(D)** Maintenance: Surgery and IA20%2BC
1098 timeline. Mice first underwent IA20%2BC for 7 weeks. Groups were balanced based on average
1099 daily alcohol consumption in last 6 drinking sessions. Mice received a bilateral, dual-infusion of

1100 AAV-Rac1-DN or AAV-GFP as a control and were allowed one full week for recovery. IA20%2BC
1101 resumed for 4 weeks. **(E)** Weekly average consumption (g/kg/24hrs.) for maintenance drinking
1102 mice. **(F)** Preference for alcohol for maintenance-drinking mice. All data represented as
1103 mean ± SEM and analyzed with two-way ANOVA with repeated measures. n = 9-10.
1104
1105 **Figure 9. Rac1 in the DMS is required for alcohol-associated goal-directed learning**
1106 **(A)** Operant self-administration of 20% alcohol paradigm. Mice underwent surgery to overexpress
1107 AAV-Rac1-DN or AAV-GFP in the DMS. After 3 weeks of recovery, mice underwent 7 weeks of
1108 IA20%2BC to develop a preference for alcohol before transitioning to 20% alcohol OSA for 1
1109 week of training and 4 experimental weeks. **(B-C)** The group average of active **(B)** and inactive
1110 **(C)** lever presses during the 2-hour sessions. **(D)** Discrimination index for the active lever.
1111 Calculated as proportion of active lever presses compared to total lever presses. **(E)** Proportion
1112 of rewarded lever presses. Calculated as rewarded lever presses compared to total lever presses.
1113 **(F)** Alcohol consumption during each session. **(G)** Proportion of inter-response interval between
1114 lever presses during the final session. Data are presented as mean ± SEM and analyzed using
1115 RM Two-way ANOVA and Šidák's *post hoc* multiple comparisons test. *p<0.05, **p<0.01,
1116 ***p<0.001. n = 6, 7. **(H)** Individual mouse behavioral profiles from OSA session 9. Each line
1117 corresponds with an active (green) or inactive (red) lever press, and triangles represent reward
1118 (purple). **(I)** Total distance moved in an open field. Mice were placed in an open field and
1119 locomotion was recorded for 20 minutes. Data represented as mean ± SEM and analyzed using
1120 an unpaired t-test. n = 9 per group.
1121
1122 **Figure 10. Rac1 in the DMS is not required for sucrose goal-directed learning**
1123 **(A)** Operant self-administration of 1% sucrose paradigm. Mice underwent surgery to overexpress
1124 AAV-Rac1-DN or AAV-GFP in the DMS. After 3 weeks of recovery, mice were age matched to
1125 20% alcohol OSA mice by waiting 7 weeks. 1% sucrose OSA began with 1 week of training and

1126 4 weeks of experimental tracking. Variables tracked during the session include **(B)** active lever
1127 presses and **(C)** inactive lever presses. **(D)** Discrimination and **(E)** proportion of rewarded lever
1128 presses were calculated. Data are represented as mean ± SEM and analyzed using RM Two-Way
1129 ANOVA. n = 7, 6.
1130
1131 **Extended Figure 1. Rac1 is activated after 4 weeks of IA20%2BC in male mice**
1132 **(A)** Mice underwent IA20%2BC in the home cage for 4 weeks before dissection during withdrawal.
1133 **(B)** After 4 weeks of IA20%2BC, the DMS was harvested and Rac1-GTP pull-down assay was
1134 conducted on cell lysates. Levels of GTP-bound Rac1 were normalized to total Rac1 and
1135 presented as percentage of the average of the water values. Data are represented as
1136 mean ± SEM and analyzed with an unpaired two-tailed t-test. *$p < 0.05$. n = 4 per group.
1137
1138 **Extended Figure 2. Characterization of AAV-2 expressing dominant negative Rac1**
1139 **(A)** HEK293 cells infected with AAV-Rac1-DN imaged in both brightfield and GFP to detect viral
1140 infection (2X magnification). **(B)** Western blot analysis of Rac1 protein in non-infected cells and
1141 cells infected with AAV-Rac1-DN. **(C)** Western blot analysis of phospho-LIMK in non-infected cells
1142 and cells infected with AAV-Rac1-DN after stimulation with 10% FBS. **(D)** Western blot of the
1143 phosphorylation of ERK1/2 in non-infected cells and cells infected with AAV-Rac1-DN after
1144 stimulation with 10% FBS. **(E-F)** Left images (4X magnification) depict the specificity of the
1145 infection site for AAV-GFP **(E)** and AAV-Rac1-DN **(F)**, scale bar 500μm. Right images (20X
1146 magnification) depict solely neurons infected in the DMS by both AAV-GFP **(E)** and AAV-Rac1-
1147 DN **(F)**, scale bar 100μm. Each slice is stained with anti-GFP (green) and anti-NeuN (red)
1148 antibodies, along with DAPI (magenta). **(G)** Mice were infected with AAV-GFP or AAV-Rac1-DN
1149 before undergoing IA20%2BC as described in Figure 5A. The DMS was harvested, and total Rac1
1150 protein level was examined using western blot and normalized to GAPDH. Data are presented as

1151 mean ± SEM and analyzed using two-way ANOVA with *post hoc* Šidák's multiple comparisons

1152 test. ***p<0.001 ****p<0.0001; ns, non-significant. n = 6 per group.

1153

1154 **Extended Figure 3. Inhibition of Rac1 in the DMS does not alter water consumption (A-B)**

1155 Water consumption averages for the IA20%2BC development **(A)** and maintenance **(B)** drinking

1156 groups. Data presented as mean ± SEM and analyzed using RM Two-way ANOVA. n = 9-10.

Figure 1

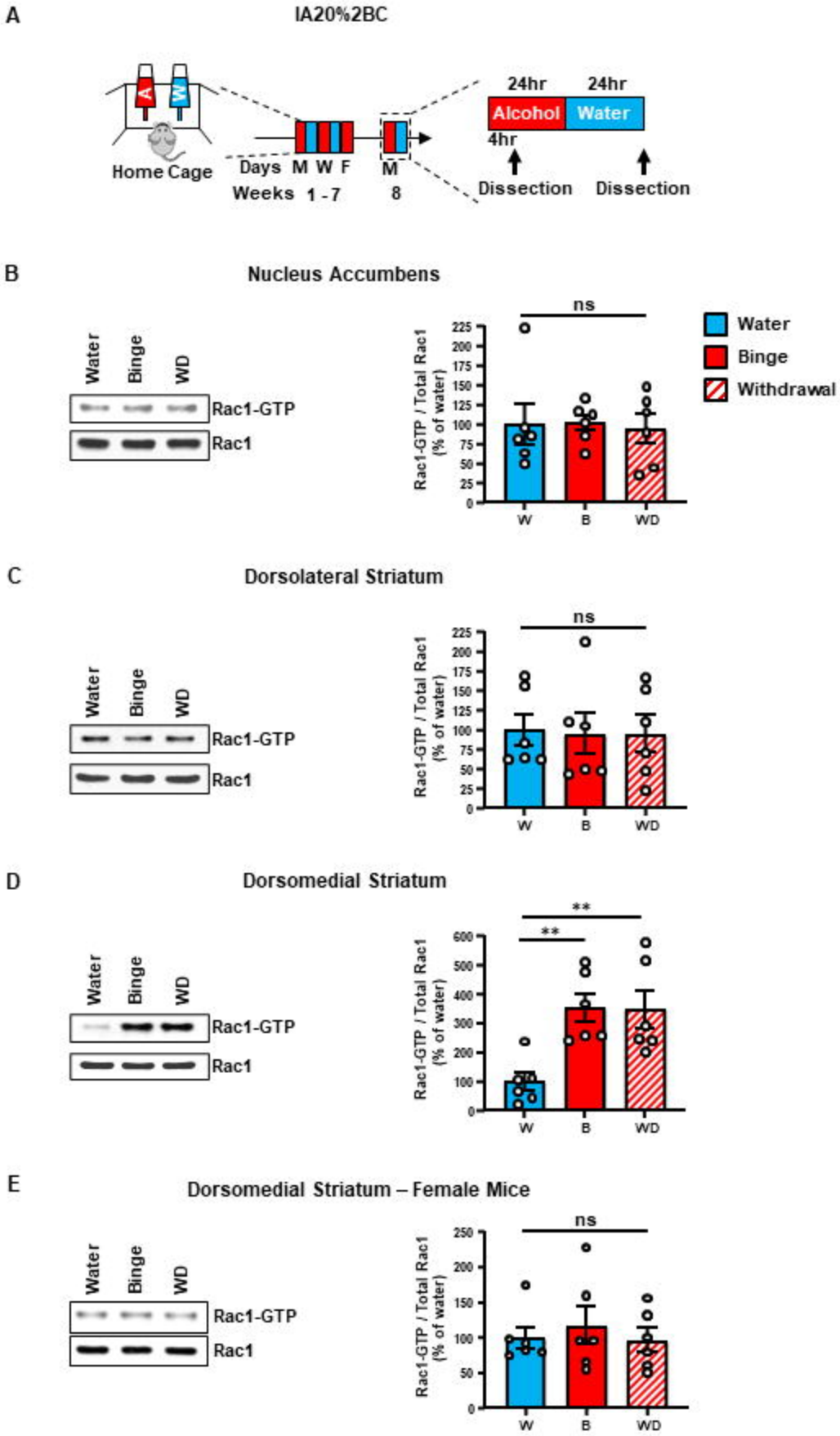
A
IA20%2BC
Home Cage
Days M W F
Weeks 1 - 7
M
8
24hr
24hr
Alcohol
Water
4hr
Dissection
Dissection
B
Nucleus Accumbens
Water
Binge
WD
Rac1-GTP
Rac1
ns
Rac1-GTP / Total Rac1 (% of water)
W
B
WD
Water
Binge
Withdrawal
C
Dorsolateral Striatum
D
Dorsomedial Striatum
**
E
Dorsomedial Striatum – Female Mice

Figure 2

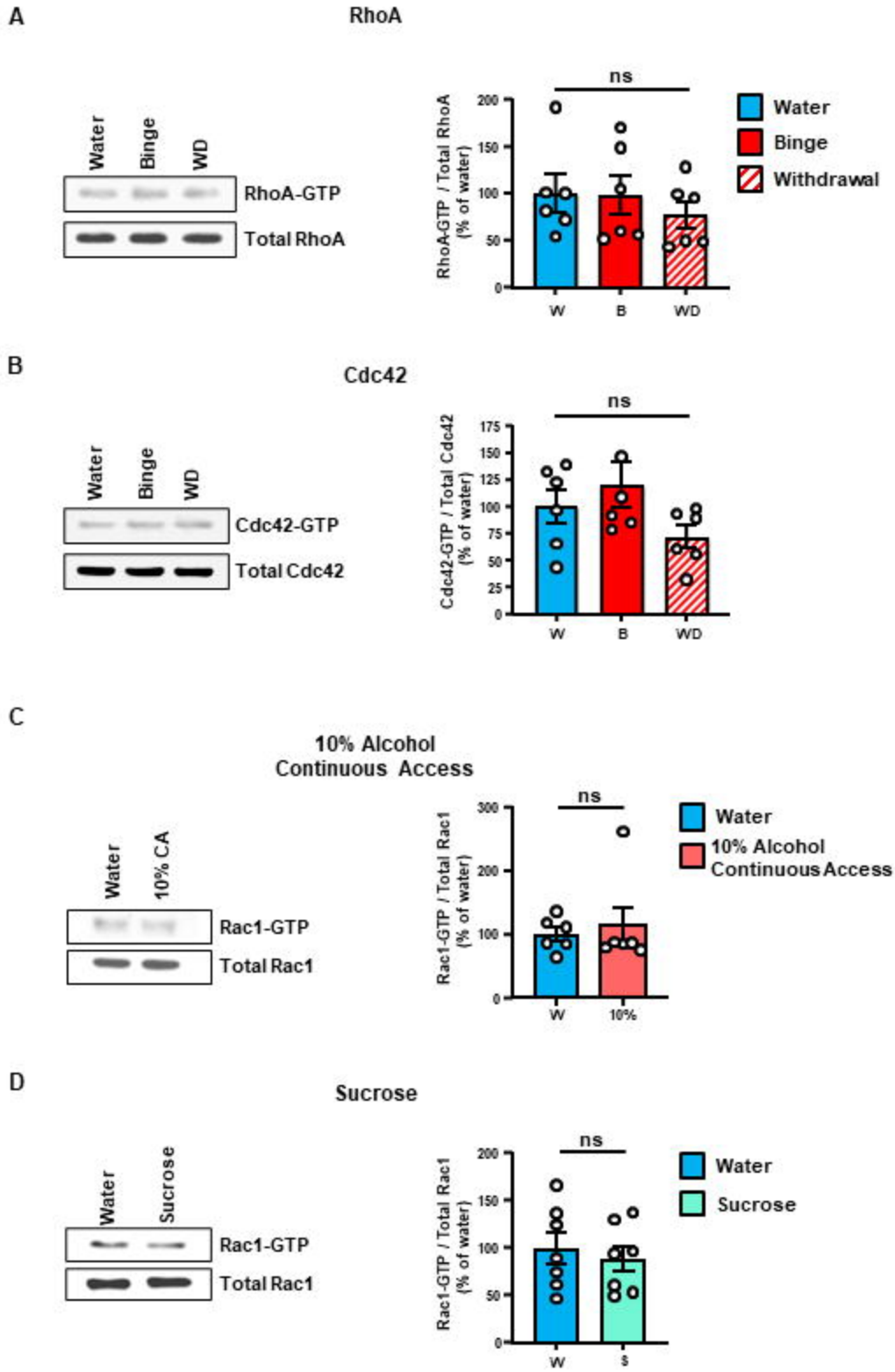
A
RhoA
Water
Binge
WD
RhoA-GTP
Total RhoA
ns
RhoA-GTP / Total RhoA (% of water)
200
150
100
50
0
W
B
WD
Water
Binge
Withdrawal
B
Cdc42
Water
Binge
WD
Cdc42-GTP
Total Cdc42
ns
Cdc42-GTP / Total Cdc42 (% of water)
175
150
125
100
75
50
25
0
W
B
WD
C
10% Alcohol
Continuous Access
Water
10% CA
Rac1-GTP
Total Rac1
ns
Rac1-GTP / Total Rac1 (% of water)
300
200
100
0
W
10%
Water
10% Alcohol
Continuous Access
D
Sucrose
Water
Sucrose
Rac1-GTP
Total Rac1
ns
Rac1-GTP / Total Rac1 (% of water)
200
150
100
50
0
W
S
Water
Sucrose

Figure 3

A

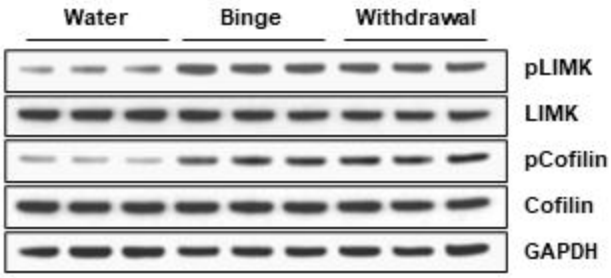
Water
Binge
Withdrawal
pLIMK
LIMK
pCofilin
Cofilin
GAPDH

B

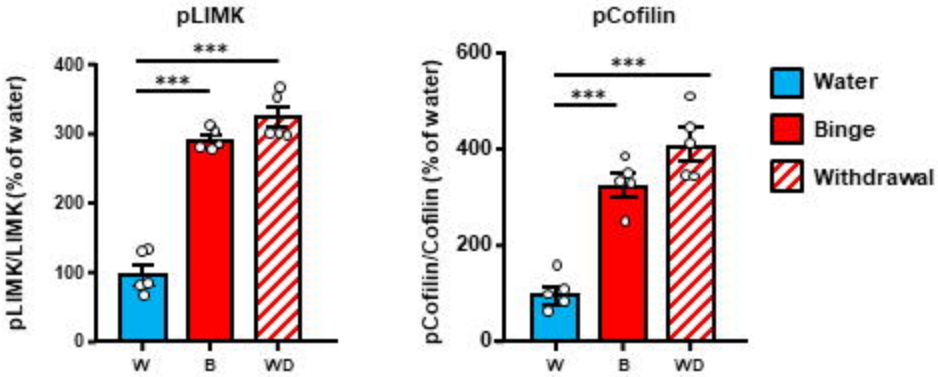
pLIMK
pLIMK/LIMK (% of water)
400
300
200
100
0
***
***
W
B
WD
pCofilin
pCofilin/Cofilin (% of water)
600
400
200
0
***
***
W
B
WD
Water
Binge
Withdrawal

Figure 4

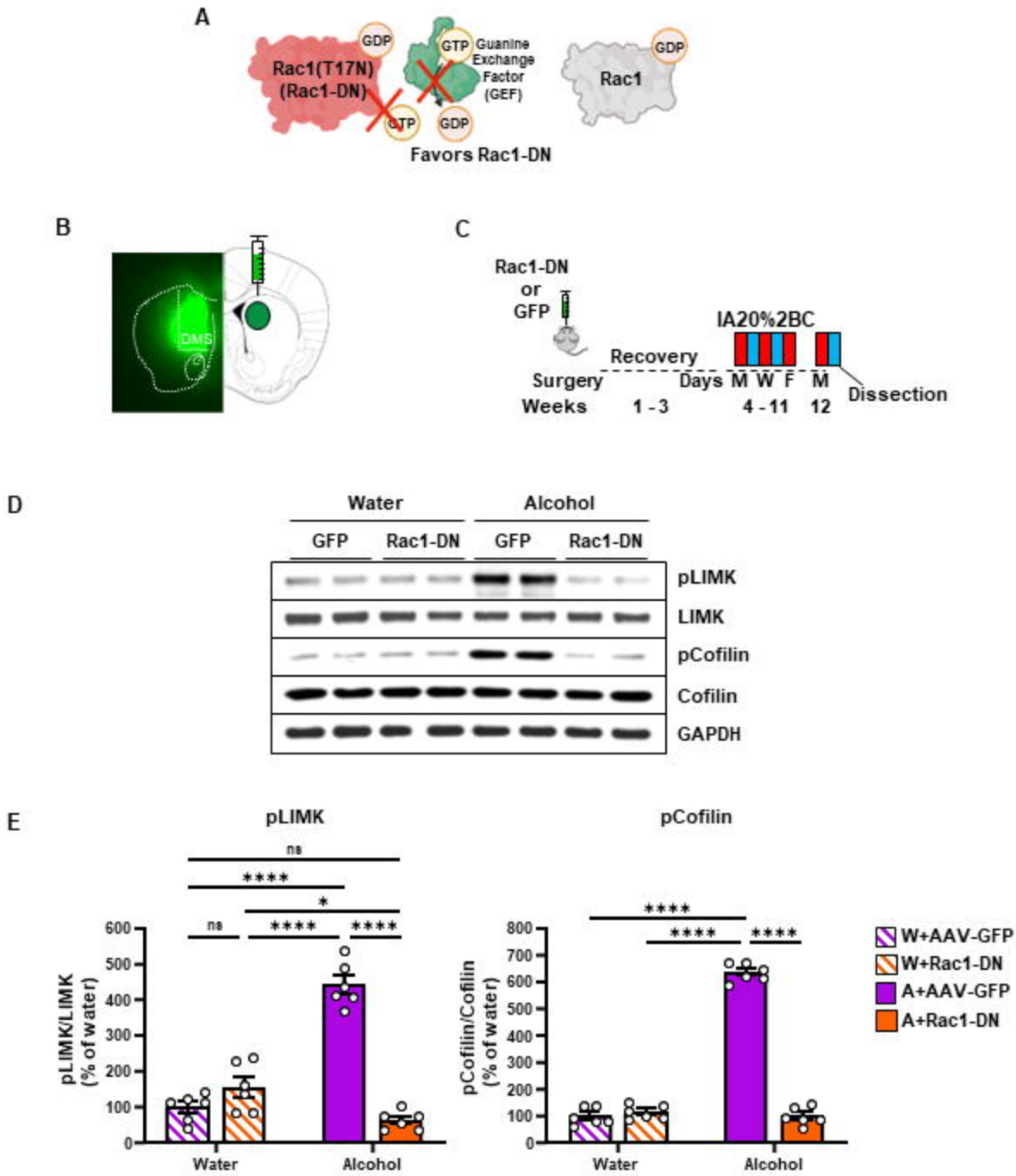
A
Rac1(T17N)
(Rac1-DN)
GDP
GTP
GTP
GDP
Guanine
Exchange
Factor
(GEF)
Rac1
GDP
Favors Rac1-DN
B
DMS
C
Rac1-DN
or
GFP
Recovery
IA20%2BC
Surgery
Days M W F M
Weeks 1 - 3 4 - 11 12
Dissection
D
Water
Alcohol
GFP
Rac1-DN
GFP
Rac1-DN
pLIMK
LIMK
pCofilin
Cofilin
GAPDH
E
pLIMK
pCofilin
ns
****
*
ns
****
****
****
****
****
pLIMK/LIMK
(% of water)
pCofilin/Cofilin
(% of water)
0
100
200
300
400
500
600
700
800
Water
Alcohol
W+AAV-GFP
W+Rac1-DN
A+AAV-GFP
A+Rac1-DN

Figure 5

A

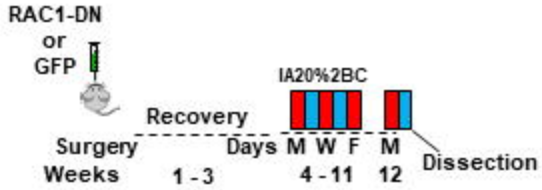
RAC1-DN
or
GFP
IA20%2BC
Recovery
Surgery
Days M W F M
Weeks
1 - 3
4 - 11
12
Dissection

B

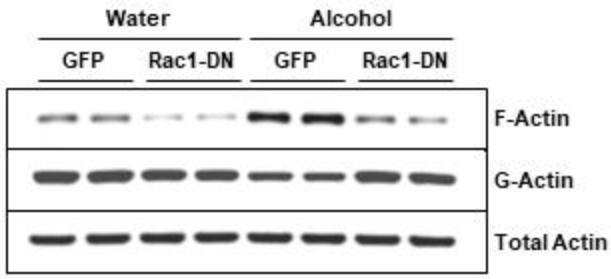
Water
Alcohol
GFP
Rac1-DN
GFP
Rac1-DN
F-Actin
G-Actin
Total Actin

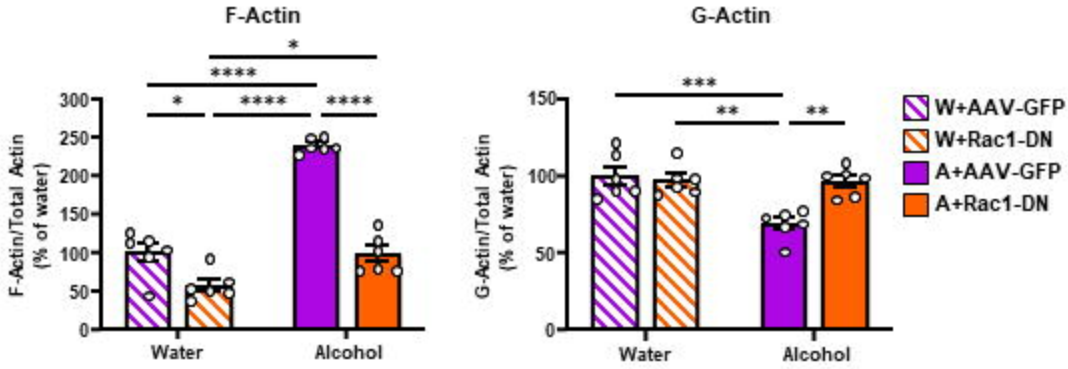
F-Actin
G-Actin
F-Actin/Total Actin
(% of water)
G-Actin/Total Actin
(% of water)
300
250
200
150
100
50
0
Water
Alcohol
*
****
*
****
****
***
**
**
W+AAV-GFP
W+Rac1-DN
A+AAV-GFP
A+Rac1-DN

Figure 6

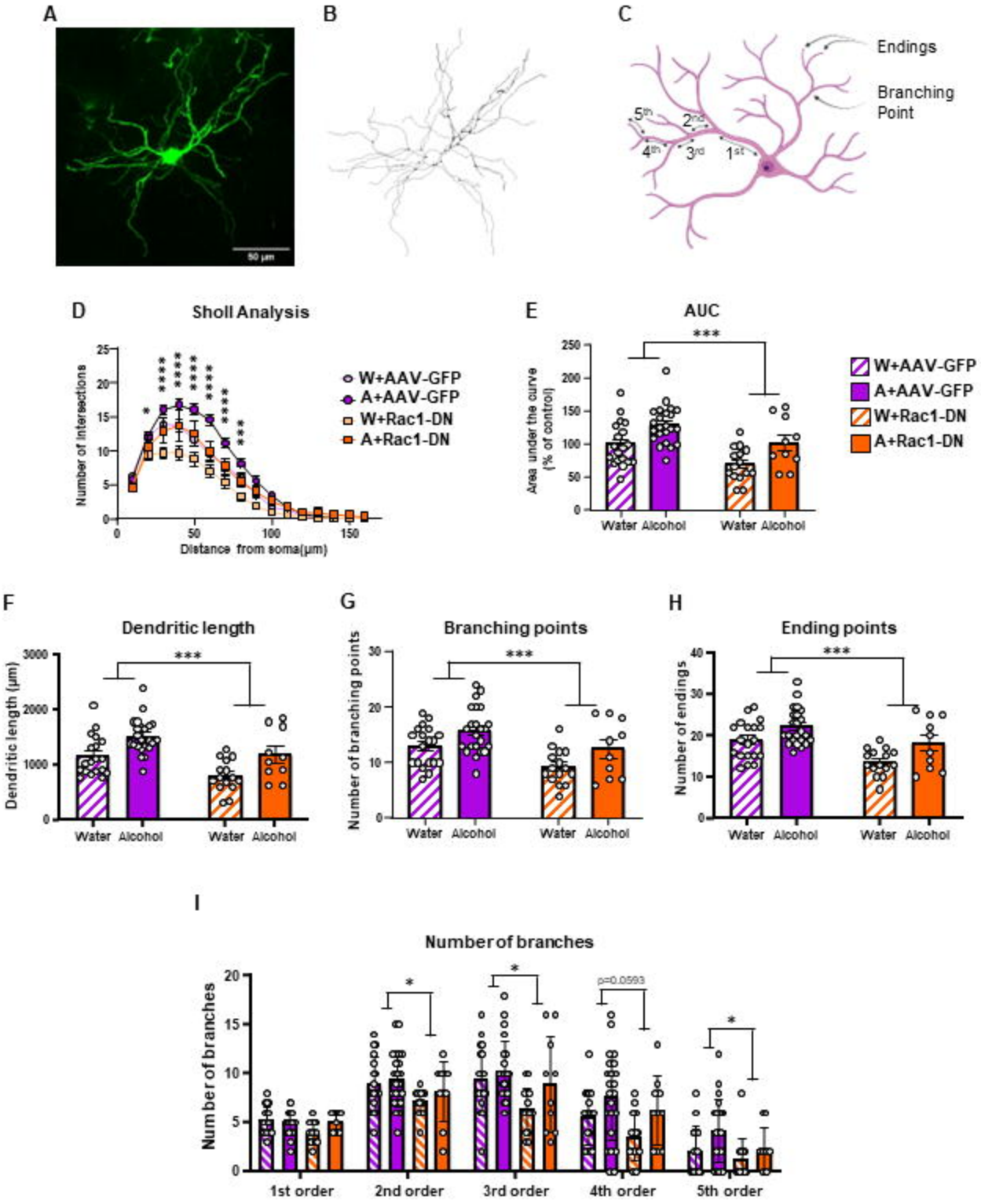
A
50 µm
B
C
Endings
Branching Point
5th
2nd
4th
3rd
1st
D
Sholl Analysis
Number of intersections
Distance from soma(µm)
W+AAV-GFP
A+AAV-GFP
W+Rac1-DN
A+Rac1-DN
E
AUC
Area under the curve (% of control)
Water
Alcohol
F
Dendritic length
Dendritic length (µm)
G
Branching points
Number of branching points
H
Ending points
Number of endings
I
Number of branches
Number of branches
p=0.0593
1st order
2nd order
3rd order
4th order
5th order

Figure 7

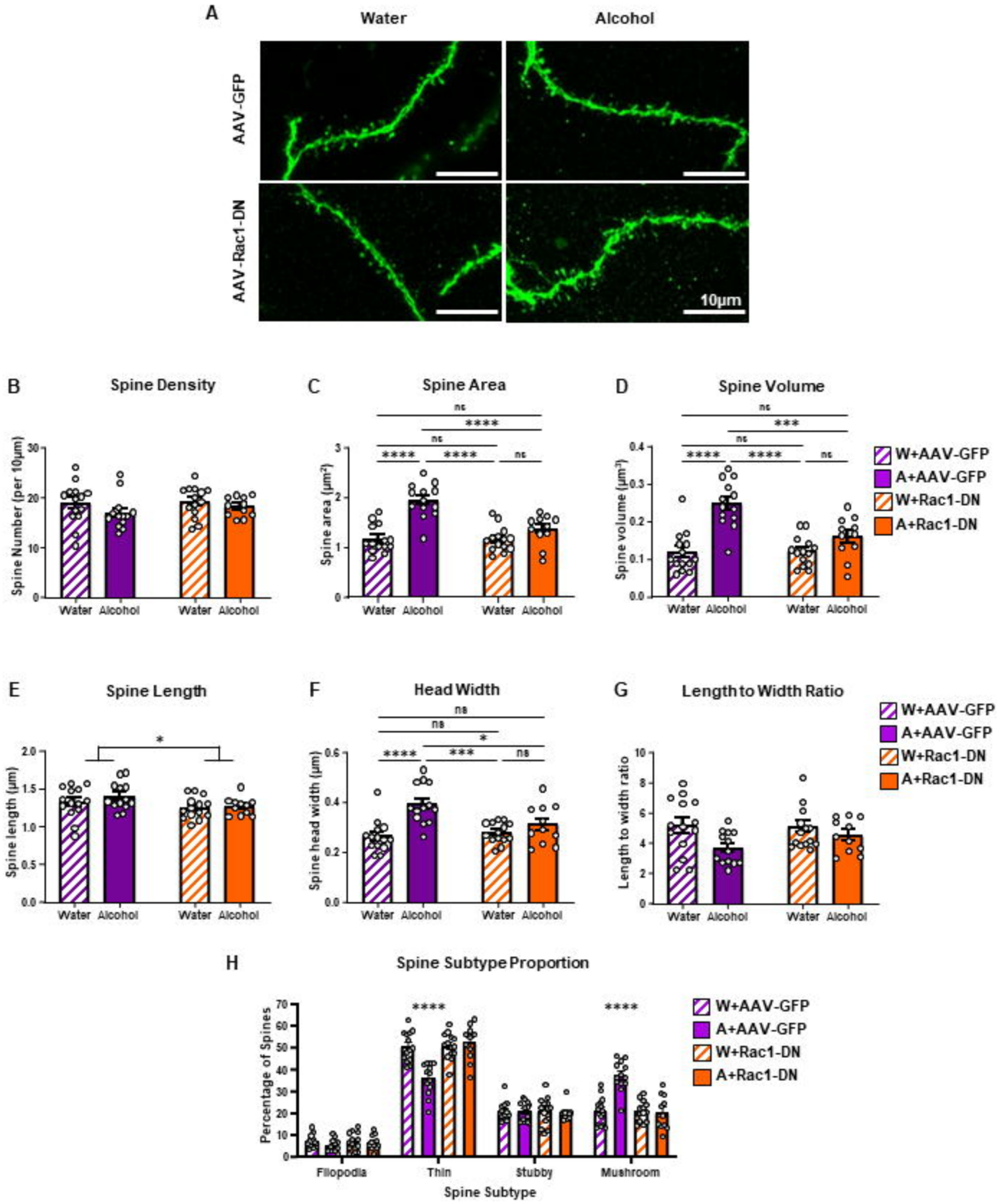
A
Water
Alcohol
AAV-GFP
AAV-Rac1-DN
10μm
B
Spine Density
Spine Number (per 10μm)
Water
Alcohol
C
Spine Area
Spine area (μm²)
ns
****
***
D
Spine Volume
Spine volume (μm³)
W+AAV-GFP
A+AAV-GFP
W+Rac1-DN
A+Rac1-DN
E
Spine Length
Spine length (μm)
*
F
Head Width
Spine head width (μm)
G
Length to Width Ratio
Length to width ratio
H
Spine Subtype Proportion
Percentage of Spines
Filopodia
Thin
Stubby
Mushroom
Spine Subtype

Figure 8

A

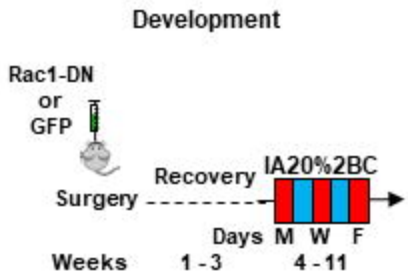

B

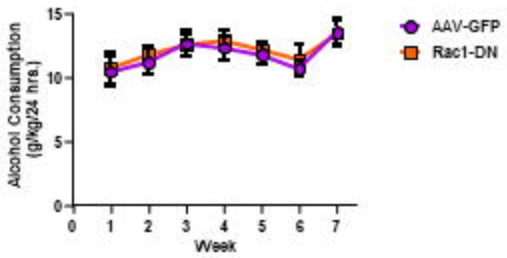

C

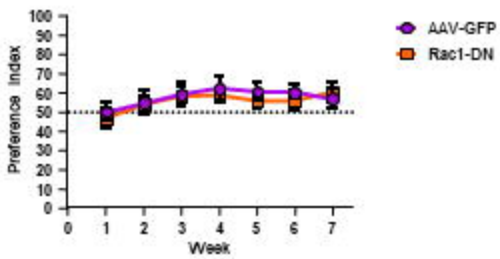

D

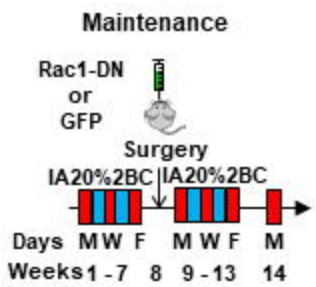

E

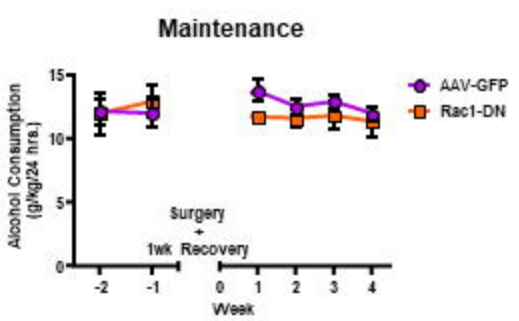

F

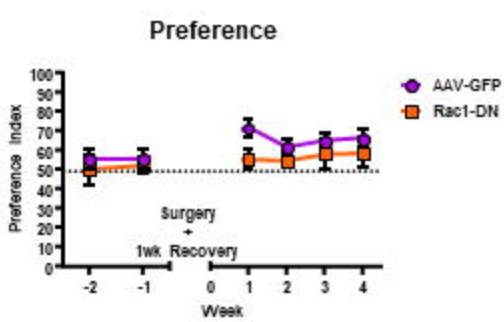

Figure 9

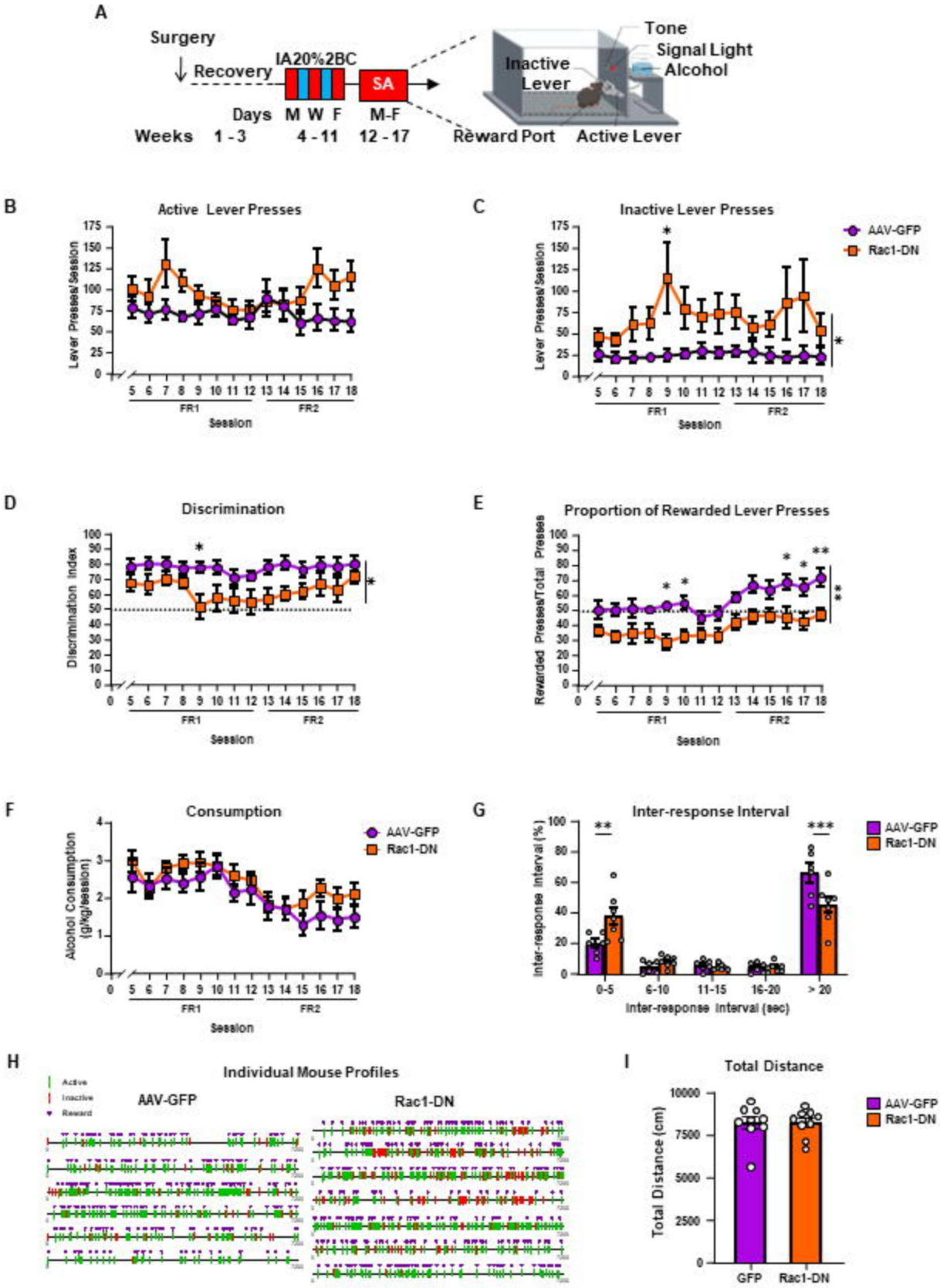
A
Surgery
Recovery
IA20%2BC
SA
Days M W F M-F
Weeks 1 - 3 4 - 11 12 - 17
Tone
Signal Light
Alcohol
Inactive Lever
Reward Port
Active Lever
B
Active Lever Presses
Lever Presses/Session
Session
FR1
FR2
C
Inactive Lever Presses
AAV-GFP
Rac1-DN
D
Discrimination
Discrimination Index
E
Proportion of Rewarded Lever Presses
Rewarded Presses/Total Presses
F
Consumption
Alcohol Consumption (g/kg/session)
G
Inter-response Interval
Inter-response Interval (%)
Inter-response Interval (sec)
0-5
6-10
11-15
16-20
> 20
H
Individual Mouse Profiles
Active
Inactive
Reward
AAV-GFP
Rac1-DN
I
Total Distance
Total Distance (cm)
GFP
Rac1-DN

Figure 10

A

B

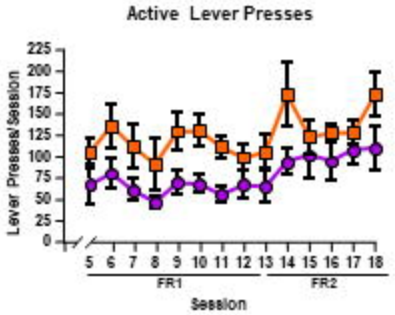

C

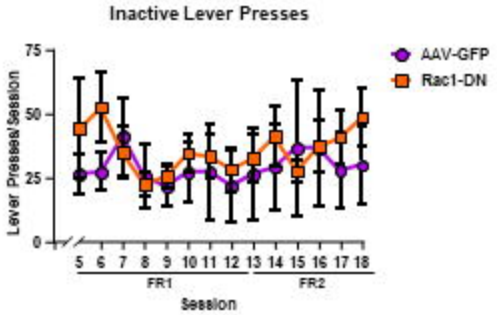

D

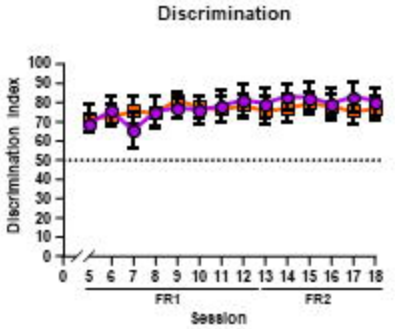

E

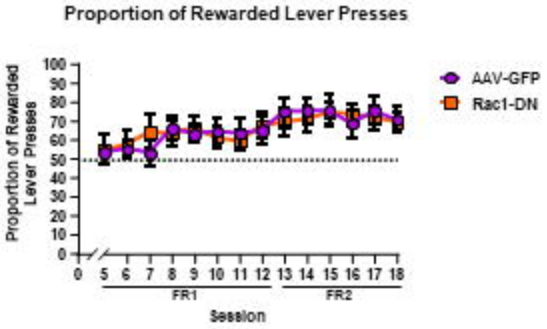

Extended Figure 1

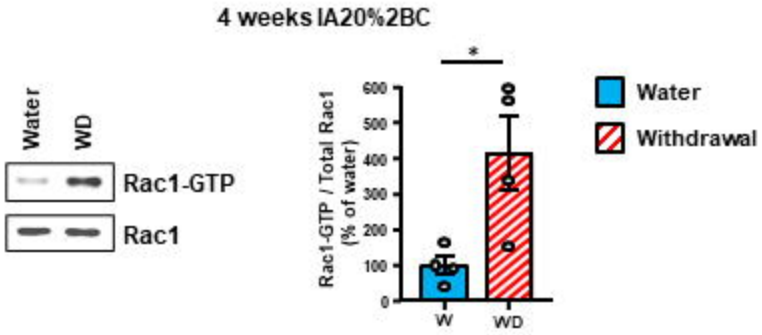

Extended Figure 2

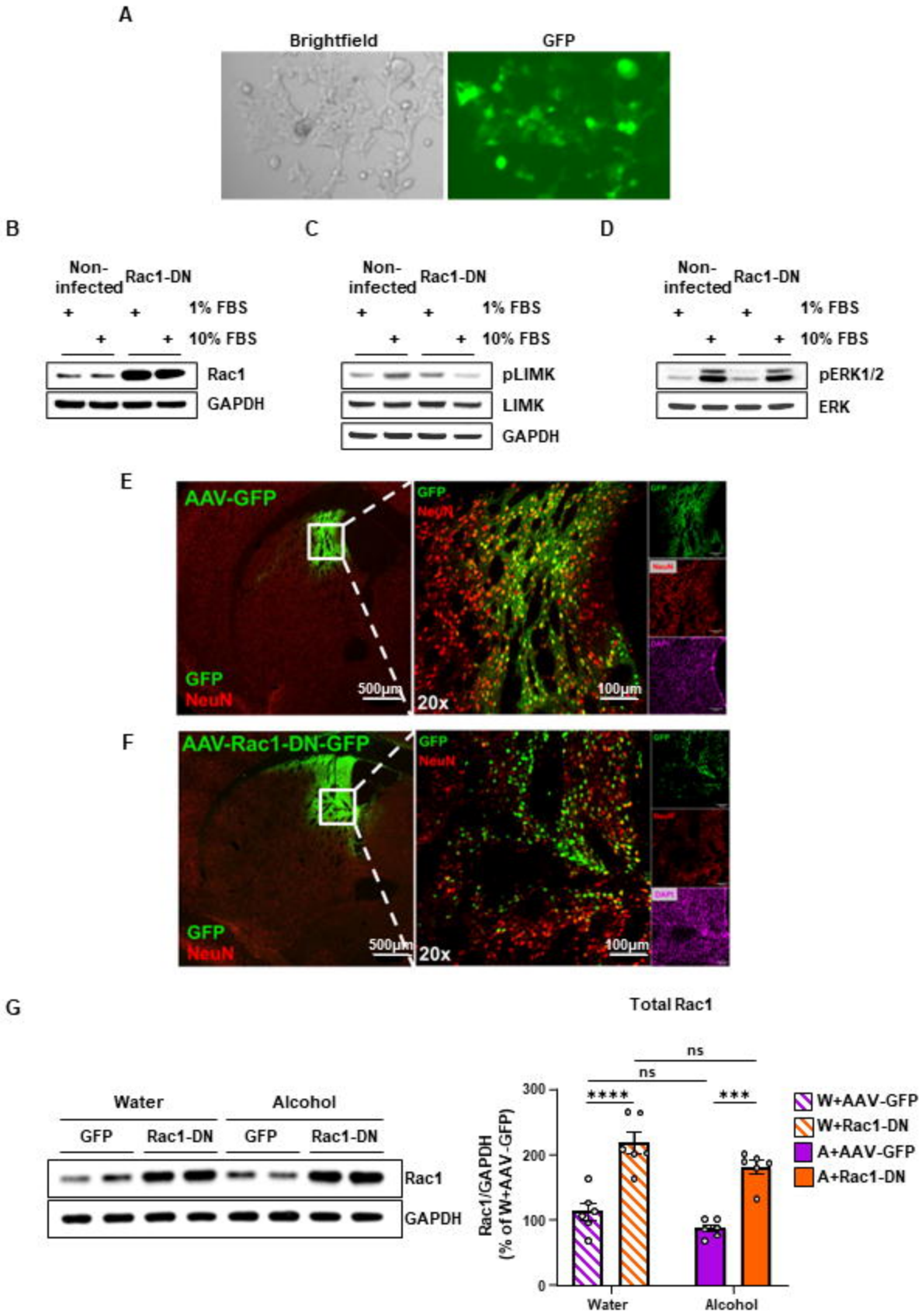
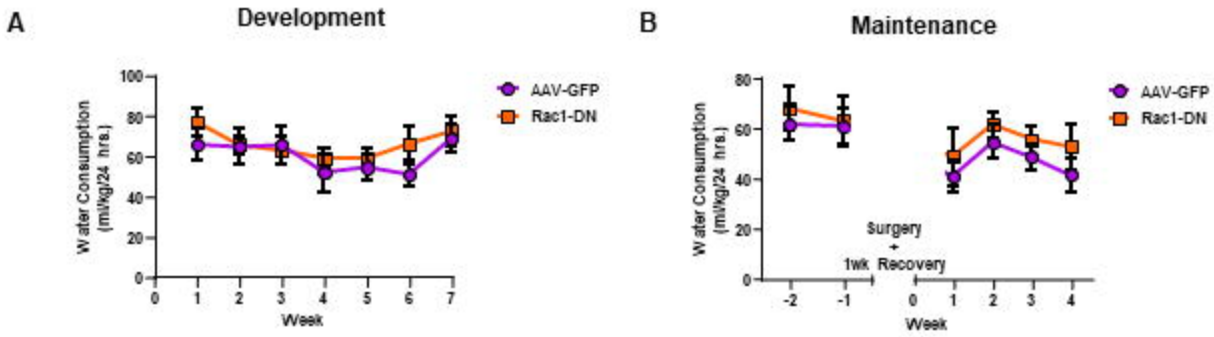
Extended Figure 3